Actively replicating gut bacteria identified by 5-ethynyl-2'-deoxyuridine (EdU) click chemistry and cell sorting

Eve T. Beauchemina[a], Claire Hunter[b], & Corinne F. Maurice[c]

[a]Department of Microbiology & Immunology, Faculty of Medicine and Health Sciences, McGill University, Montreal, Quebec, Canada. eve.beauchemin@mail.mcgill.ca

[b]Department of Microbiology & Immunology, Faculty of Medicine and Health Sciences, McGill University, Montreal, Quebec, Canada.

[c]Department of Microbiology & Immunology, Faculty of Medicine and Health Sciences, McGill University, Montreal, Quebec, Canada. corinne.maurice@mcgill.ca

Corresponding Author: Corinne F. Maurice

Email address: corinne.maurice@mcgill.ca

Abstract

The composition of the intestinal bacterial community is well described, but recent research suggests that the metabolism of these bacteria plays a larger role in health than which species are present. One fundamental aspect of gut bacterial metabolism that remains understudied is bacterial replication. Indeed, there exist few techniques which can identify actively replicating gut bacteria. In this study, we aimed to address this gap by adapting 5-ethynyl-2'-deoxyuridine (EdU) click chemistry (EdU-click), a metabolic labeling method, coupled with fluorescence-activated cell sorting and sequencing (FACS-Seq) to characterize replicating gut bacteria. We first used EdU-click with human gut bacterial isolates and show that many of them are amenable to this technique. We then optimized EdU-click and FACS-Seq for murine fecal bacteria and reveal that *Prevotella* UCG-001 and *Ileibacterium* are enriched in the replicating fraction. Finally, we labelled the actively replicating murine gut bacteria during exposure to cell wall-specific antibiotics *in vitro*. We show that regardless of the antibiotic used, the actively replicating bacteria largely consist of *Ileibacterium*, suggesting the resistance of this taxon to perturbations. Overall, we demonstrate how combining EdU-click and FACSeq can identify the actively replicating gut bacteria and their link with the composition of the whole community in both homeostatic and perturbed conditions. This technique will be instrumental in elucidating *in situ* bacterial replication dynamics in a variety of other ecological states, including colonization and species invasion, as well as for investigating the relationship between the replication and abundance of bacteria in complex communities.

Keywords

Click chemistry; gut microbiota; bacterial physiology; bacterial replication; EdU; 5-ethynyl-2'-deoxyuridine; flow cytometry; cell sorting

Introduction

The community of microorganisms which reside in the intestines of animals, called the gut microbiota, forms one of the densest and most diverse microbial assemblages in the world. The gut microbiota primarily consists of bacteria and the viruses that infect them, with lesser numbers of archaea, fungi, and other eukaryotic microorganisms.[1-4] Due to their numerical dominance and the existence of tools to study them, bacteria are the best characterized microorganisms in the gut. Among many other roles, these bacteria help to train the immune system, prevent pathogen invasion, and break down indigestible fibers into host-accessible metabolites[4-7].

Most studies on the gut microbiota to date have focused on describing which bacteria are present in the gut and tried to decipher their links with disease. In recent years, however, more studies have been focusing on additionally describing the activity of these microorganisms.[1,8-12] Indeed, the metabolism of the gut bacteria has been suggested to play a bigger role in determining the health status of their host than composition alone.[1,13] Furthermore, studying the *in situ* physiology of bacterial communities is suggested to provide a more detailed and accurate picture of how microbiotas function and interact within themselves and with their (host) environment, as compared to culture- or sequence-based methods.[14]

One aspect of microbial physiology which is of growing interest is bacterial replication. The replication strategies of individual gut microbial members have been shown to impact the overall functional capacity of the community and could allow the description and prediction of the

63 outcomes of ecological processes such as competition, succession, and extinction events.[15,16]
64 Several techniques in the fields of systems biology and bioinformatics have recently been
65 developed to quantify the replication dynamics of specific gut bacterial taxa or all bacterial
66 members within the gut community, respectively.[17-19] Notably, the bioinformatics-based studies
67 report correlations between bacterial replication rates and diverse host health parameters, including
68 the occurrence of type II diabetes and inflammatory bowel disease[20,21]. Furthermore, some of the
69 systems biology approaches have shown that *Escherichia coli* replication dynamics in the gut are
70 altered during host inflammation,[19] and that a murine *E. coli* strain successfully colonizes the gut
71 in part by dividing twice as fast as it is removed.[18]

72 However, there exist fewer physiological methods for measuring the replication of individual
73 bacteria in complex communities *in situ*. The recently developed fluorescent labeling of newly
74 synthesized bacterial peptidoglycan is a purely qualitative approach, which also requires the
75 creation of modified probes to allow for fluorescent *in situ* hybridization to taxonomically identify
76 labeled bacteria, a non-trivial task.[22-25] Quantitative stable isotope probing of bacterial DNA
77 (DNA-qSIP) is time- and resource-intensive.[16] However, it is compatible with downstream
78 methods to separate and sequence the DNA of labeled cells, which allows the replication rates of
79 individual taxa to be estimated.[16] This process of labeling, sorting, and characterizing active
80 bacteria is becoming more and more popular due to its unparalleled ability to link bacterial
81 metabolism and identity.[14,26]

82 One physiological method for labeling replicating bacteria, which has not yet been used with the
83 gut microbiota, are thymidine analogues. New thymidine analogues which use fluorescent probes
84 are easier and safer to use than their older radioactive counterparts, especially in the context of
85 probing environmental communities *in situ*.[27,28] This is especially the case for the thymidine

86 analogue 5-ethynyl-2'-deoxyuridine (EdU), which uses the reliable, quick, and simple method of
87 'click' chemistry (EdU-click) to fluorescently label incorporated EdU in newly created strands of
88 DNA .[27] Like qSIP, it can be paired with downstream methods to sort and sequence the labeled
89 cells, providing taxonomic information on the replicating and non-replicating communities. To
90 date, however, EdU-click has only been used once in a complex aquatic microbial community. In
91 this context, the researchers identified that between 4.4 to 49% of bacteria in coastal waters were
92 replicating, with a low number of cells contributing to the majority of the fluorescence signal.[29] If
93 modified, this approach could be used to investigate the replication dynamics of the gut microbiota.
94 For instance, this technique could help determine whether bacterial replication is a phylogenetic
95 characteristic in the gut, as it is suggested to be in soil communities,[30] or whether it is a dynamic
96 feature of bacterial metabolism which can change with fluctuating environmental conditions.

97 We here describe the use of the EdU-click technique first in select gut bacterial isolates, followed
98 by optimization of the procedure for the murine gut microbiota. We then combine this technique
99 with fluorescence-activated cell sorting (FACS) and 16S amplicon sequencing (FACS-Seq) to
100 physically separate and taxonomically identify the replicating bacterial communities in healthy
101 mice. We end by demonstrating one potential application of the optimized EdU-click and FACS-
102 Seq procedure, to identify the replicating gut bacteria after an *in vitro* antibiotic exposure. Our
103 findings reveal that many gut bacterial isolates are amenable to EdU-click, and that the replicating
104 gut bacteria in healthy mice is dominated by *Ileibacterium*. We additionally report that exposure
105 of mouse fecal bacteria to an antibiotic either targeting Gram-negative or Gram-positive bacteria
106 results in an increased presence of *Ileibacterium* in the replicating fraction of the gut.

107

108 **Results**

109 ***Optimization of EdU-click in gut bacterial isolates***

110 To determine whether EdU could be incorporated into phylogenetically distinct bacteria, we first
111 performed EdU-click followed by flow cytometry (**Fig. 1a**) on nine gut bacterial isolates, spanning
112 five phyla and the two cell wall types: *Bacteroides caccae, Bacteroides fragilis*, and *Prevotella*
113 *intermedia* (Bacteroidetes, Gram -)*; Clostridium beijerinckii*, *Enterococcus faecalis*, and
114 *Ruminococcus bromii* (Firmicutes, Gram +); *Bifidobacterium longum* subsp. *infantis*
115 (Actinobacteria, Gram +); *Escherichia coli* K12 (Proteobacteria, Gram -); and *Akkermansia*
116 *muciniphila* (Verrucomicrobia, Gram -).

117 Bacterial isolates were incubated anaerobically at 37 °C with or without 20 µm EdU in reduced
118 Bovine Heart Infusion broth (BHI) for three hours. Cells were then fixed and underwent the click
119 and flow cytometry procedures as described in the Methods. Duplicates of each isolate incubated
120 without EdU served as controls to set up the gating strategy (see **Figs 1b, c; S1**). The different
121 bacterial isolates exhibited varying proportions of EdU^+ cells, quantified relative to all bacterial
122 cells obtained after SybrGreen staining (see Methods). Specifically, 34.38% ± 17.67 of *P.*
123 *intermedia* cells, 43.97% ± 6.51 of *C. beijerinckii* cells, 98.7% ± 0.09 of *E. faecalis* cells, and
124 98.66% ± 0.31 of *E. coli* cells were labeled with EdU, whereas no cells of *B. fragilis*, *B. caccae,*
125 *R. bromii, B. infantis,* or *A. muciniphila* were labeled during the same growth period (**Fig. 1b, d;**
126 **Fig. S1a**). Heat-killed *E. coli* K12 cells which underwent the EdU-click procedure did not label
127 (**Fig. S2**), demonstrating that only actively replicating bacteria are labelled using this technique.

128 It is unclear why some isolates did not label with EdU, despite exhibiting growth (**Fig. S1b**). It is
129 not likely due to differences in cell wall type, since both Gram-positive (*E. faecalis, C. beijerinckii*)
130 and Gram-negative (*E. coli, P. intermedia*) representatives were similarly labeled with EdU.
131 Differences in growth rates may be implicated, as correlation analyses between the proportion of

132 EdU^+ cells and the maximal replicate rate (Max V) revealed a significant positive correlation
133 (Pearson $r^2 = 0.407$, $p = 0.0005$) for these isolates (**Fig. S1c**). This correlation was stronger when
134 *B. infantis*, the only fast-growing isolate unlabeled with EdU, was removed from the analysis ($r^2 =$
135 0.6019, $p < 0.0001$, **Fig. S1d**). Other possible reasons for the lack of labeling of these isolates are
136 explored in more detail in the Discussion.

137 We further confirmed the fluorescence signals of these isolates by epifluorescence microscopy
138 (**Fig 1b, c; Fig. S3**), validating the detected signal obtained by flow cytometry. Previous studies
139 in *E. coli* have verified the specificity of EdU in labeling newly created DNA, and no other cell
140 components.[31,32]

141 ***EdU-click validation in mouse fecal bacteria***

142 We next sought to determine if EdU-click could be used to identify replicating bacteria in a
143 complex microbial community, using fecal samples from healthy C57BL/6 mice.

144 We first tested incremental EdU concentrations from 10 to 100 μM on resuspended bacterial
145 communities from mouse fecal samples, or mouse fecal bacteria, in three independent experiments
146 (N= 4-5 mice per experiment, see Methods; **Fig 2a, Fig. S4**). The proportion of EdU^+ cells varied
147 according to the cohort of mice, limiting the direct comparison of proportions of EdU^+ cells
148 between experiments. In each independent experiment, the proportions of EdU^+ cells increased in
149 a concentration-dependent manner and were only significantly lower at 10 μM EdU relative to
150 higher concentrations in one experiment ($p < 0.05$, Kruskal-Wallis with post-hoc Dunn's multiple
151 comparisons test, **Fig. S4a**). We report a non-significant increase in EdU^+ cells with EdU
152 concentrations between 10-35 μM (**Fig. 2a**), and between 20-80 μM (**Fig. S4b**). Since there were

153 no large differences between these concentrations, we used the intermediate concentration of
154 20uM EdU for all downstream experiments.

155 Next, we tested two incubation media for EdU labeling of complex communities – reduced Bovine
156 Heart Infusion broth (rBHI) and a fecal slurry. Aiming to best recapitulate the host environment,
157 we performed EdU-click using each of these media either by themselves (100% rBHI or 100%
158 fecal slurry) or as various ratios of the two (3:1, 1:1, and 1:3 ratio of rBHI to fecal slurry), (**Fig.**
159 **2b**). Incubation in 100% rBHI resulted in the largest proportion of EdU^+ cells, decreasing with
160 decreasing ratios of rBHI, while incubation in pure fecal slurry did not result in any EdU labeling,
161 suggesting the slurry cannot support bacterial replication. The incubation conditions which
162 contained the most fecal slurry and similar proportions of EdU^+ cells to the rBHI were the 1:1
163 rBHI-fecal slurry medium, which is the one we selected going forward.

164 Finally, we determined the optimal incubation time with EdU. To minimize bacterial selection
165 during incubation, we chose to explore incubation times that were 3 hours or less[29,33]. We aimed
166 to determine the shortest incubation time possible which still resulted in adequate labelling for
167 downstream analyses (e.g., fluorescence-activated cell sorting). However, shorter incubation times
168 resulted in significantly lower and less clear EdU^+ signals, despite similar bacterial abundances
169 (**Fig. 2c**). We therefore proceeded with 3-hour incubations going forward.

170 We then used the optimized procedure, being a 3-hour anaerobic incubation with 20 uM EdU in
171 1:1 rBHI-fecal slurry, to label the replicating fecal bacteria in a separate cohort of mice. As seen
172 in the representative flow cytogram in **Figure 2d,** we obtained a clear population of bacterial cells
173 distinct enough to proceed with cell sorting and sequencing of the replicating cells.

174 ***EdU-click captures the actively replicating gut bacteria in healthy mice***

175 Having optimized the EdU-click protocol for mouse fecal bacteria, we next used this technique to
176 taxonomically identify the EdU^+ fraction of cells in the feces of two cohorts of mice. Mouse fecal
177 samples were obtained from a total of four cages of 4-5 mice per cage, encompassing both sexes,
178 during two independent experiments (n=17). Fecal samples from all mice in each experiment were
179 pooled before performing EdU-click to ensure enough original material for cell sorting. We then
180 used fluorescence-activated cell sorting (FACS) to separate the following bacterial fractions: (1)
181 the whole, unincubated initial community (initial community); (2) the EdU^+ cells; (3) the EdU^-
182 cells; and (4) the whole, incubated community (whole community).

183 Taxonomic identification of these sorted fractions, as well as the unsorted initial community, were
184 conducted using 16S rRNA amplicon sequencing, as described in the Methods. The unsorted
185 initial, sorted initial, and sorted whole community samples allowed us to determine possible cell
186 sorting or incubation biases. Sequences present in the sorted communities and the sheath fluid used
187 during cell sorting, but absent from the unsorted initial community, were identified as
188 contamination and manually removed from downstream analyses (see Methods). The average
189 sequencing depth of all samples (excluding the sheath fluid sample) was 24.04 Mbp (± 18.69 Mbp),
190 the average number of reads per sample was 39,926 (± 31,039), and the rarefaction curve on the
191 number of observed features found in each sample type is displayed in **Figure S5a**. After quality
192 control and filtering of contamination, the average number of reads per sample was 20,614 (±
193 14,561), with samples keeping on average 54.64% (± 14.20) of their original reads.

194 The taxonomy at the genus level of the initial community and each sorted fraction (EdU^+, EdU^-,
195 whole community) for the two experiments can be seen in **Figure 3a.** Notably, the taxonomy of
196 the initial community consisted of more species of lower-abundant bacteria as compared to the
197 sorted fractions, represented by the higher proportions of bacteria categorized as "Other".

198 Differential abundance analyses on the combined taxonomic data of both independent experiments
199 identified which bacteria were more represented in the different sorted fractions, as described in
200 the Methods. Some of the most important differentially abundant genera were, in order of
201 importance, *Akkermansia, Prevotellaceae* UCG-001, *Ileibacterium,* and *Dubosiella*.

202 *Akkermansia* and *Dubosiella* followed similar patterns, as they were both depleted in the EdU^+
203 sorted fraction despite increasing in relative abundance in the whole community. Indeed,
204 *Akkermansia* had low relative abundances in the EdU^+ fraction (experiment 1: 0.55% ± 0.21;
205 experiment 2: 2.17% ± 2.82) and the Initial community (experiment 1: 0.03% ± 0.00; experiment
206 2: 0.28% ± 0.01) relative to the Whole community (experiment 1: 1.29% ± 0.38; experiment 2:
207 2.16% ± 0.30) and the EdU^- fraction (experiment 1: 2.61% ± 0.98; experiment 2: 5.16% ± 1.73).
208 For its part, *Dubosiella* was decreased in the EdU^+ fraction (experiment 1: 2.20% ± 0.04;
209 experiment 2: 2.83% ± 3.95) as compared to the Whole community (experiment 1: 21.76% ± 6.27;
210 experiment 2: 7.25% ± 2.14) and the EdU^- fraction (experiment 1: 36.24% ± 3.41; experiment 2:
211 8.23% ± 3.77). The increased relative abundance of the taxa which are not enriched in the actively
212 replicating sorted fraction could result from the selective loss of other bacterial taxa, or could
213 indicate that only a fraction of these cells are replicating to sustain this increase. Alternatively, it
214 could suggest that despite actively replicating, they are not labeled by EdU-click, as seen in the
215 human gut isolate of *A. muciniphila* in **Figure 1d**. The *Dubosiella* species contrasts with
216 *Akkermansia*, however, in that it was already quite abundant in the initial community of
217 experiment 1 (22.54% ± 1.65) but not in experiment 2 (3.13% ± 0.06). This species may have
218 behaved differently in these two experiments due to the compositional differences of the initial
219 input community (**Fig. 2a**).

220 The relative abundance of *Prevotella* UCG-001 was increased in only the EdU^+ fraction
221 (experiment 1: 0.44% ± 0.23; experiment 2: 7.96% ± 5.83) as compared to all of the other fractions,
222 suggesting that despite being a relatively low-abundant bacteria – being present in the whole
223 community with an average relative abundance of 0.44% ± 0.23 in experiment 1 and 2.33% ± 0.75
224 in experiment 2 – many of its members are actively replicating.

225 Similarly to *Prevotella* UCG-001, the relative abundance of *Ileibacterium* was increased in the
226 EdU^+ fraction (experiment 1: 77.59% ± 2.02; experiment 2: 39.66% ± 28.72) as compared to all
227 of the other fractions. In contrast to *Prevotella* UCG-001, however, this taxon is already fairly
228 abundant in the whole community (experiment 1: 31.09% ± 1.66; experiment 2: 13.42% ± 1.27).

229 The beta diversity of these bacterial communities was visualized using Principal Coordinate
230 Analysis (PCoA) on the weighted Unifrac distance (**Fig 3b**). We excluded the EdU- sorted fraction
231 from this and subsequent analyses since it resembled the whole community taxonomically (**Fig.**
232 **3a**). We report a significant difference in the weighted Unifrac distances between the two
233 experiments (PERMANOVA, q = 0.008), as well as between the EdU^+ fraction and the whole
234 community (q = 0.018). These data support the fact that the EdU^+ fraction is enriched in specific
235 gut bacterial members.

236 When looking at the within-sample (alpha) diversity, the EdU^+ fraction had significantly lower
237 Shannon index values (Kruskal-Wallis, q = 0.029) in comparison to the other fractions for both
238 experiments (**Fig. 3ci**). The EdU^+ fraction also had a significantly lower Simpson Evenness
239 (Kruskal-Wallis, q = 0.049) relative to the whole community (**Fig. 3cii**), suggesting the numerical
240 dominance of certain taxa over others in the EdU^+ fraction. Both of these findings are corroborated

241 by the taxonomic composition of this fraction, which was enriched in certain genera and depleted
242 in others, as described above (**Fig. 3a**).

243 The initial community had a significantly higher number of observed features (Kruskal-Wallis, q
244 = 0.015) as compared to the other incubated fractions in both experiments (**Fig. 3ciii**), confirming
245 that there are a greater number of species present in the initial community relative to the incubated
246 fractions (**Fig. 3a**). The initial community also had a low Simpson evenness score (0.05 ± 0.047)
247 (**Fig 3cii**), suggesting the abundance of some species over others. This is also in agreement with
248 the taxonomy, as this fraction was typically composed of four main genera – *Muribaculaceae*
249 (experiment 1: 19.09% ± 6.02; experiment 2: 22.94% ± 4.52), *Dubosiella* (experiment 1: 22.54%
250 ± 1.65; experiment 2: 3.13% ± 0.06), *Ileibacterium* (experiment 1: 36.04% ± 6.13; experiment 2:
251 12.87% ± 1.28), and *Lachnospiraceae* NK4A136 group (experiment 1: 4.19% ± 1.44; experiment
252 2: 13.90% ± 4.36) (**Fig 3a**).

253 It is important to note that the Shannon index and Simpson Evenness metrics were significantly
254 different between the two experiments (**Fig. S6a, b**), but the number of observed features was
255 comparable (**Fig. S6c**). This is consistent with the fact that these experiments involved different
256 cages of mice from different litters, factors known to influence gut bacterial community
257 composition.[34]

258 Altogether, the diversity and taxonomic information obtained in this experiment strongly suggests
259 that the EdU^+ fraction is a specific subset of the whole gut bacterial community, enriched in
260 *Prevotella* UCG-001 and *Ileibacterium*, and depleted in *Akkermansia* and *Dubosiella*.

261 ***EdU-click reveals the replicating gut bacteria after an in vitro exposure to antibiotics***

262 After identifying the replicating bacterial taxa in healthy mice, we next sought to determine how
263 these populations would change upon an antibiotic perturbation, thereby highlighting the potential
264 of this approach *in vitro*. We thus tested the effects of polymyxin B, an antibiotic targeting Gram-
265 negative bacteria, and vancomycin, an antibiotic targeting Gram-positive bacteria, on bacteria
266 from mouse fecal samples.

267 Fecal bacteria from healthy mice were incubated in the presence of either antibiotic or only the
268 vehicle (DMSO), in addition to EdU where appropriate (see Methods). Sorting and sequencing
269 were conducted on the same fractions as previously described. The average sequencing depth of
270 all samples (excluding the sheath fluid sample) was 17.87± 12.21 Mbp, the average number of
271 reads per sample was 29,685± 10,281, and the rarefaction curve on the number of observed features
272 found in each sample type is displayed in **Figure S5b**. After quality control and filtering of
273 contamination, the average number of reads per sample was 15,495 (± 9,164), with samples
274 keeping on average 72.44% (± 14.40) of their original reads.

275 The growth curve in **Figure 4a** shows the impact of each antibiotic on the growth of mouse fecal
276 bacterial communities, and **Table SI** quantifies several characteristics of these growth curves.
277 Notably, polymyxin B resulted in a significantly longer lag time (One-Way ANOVA, $p = 0.0077$),
278 slower replication rate ($p = 0.0260$), and less overall growth ($p = 0.0013$) as compared to the control
279 (**Table SIb**). In contrast, vancomycin treatment only significantly affected total bacterial growth
280 ($p = 0.0455$) and none of the other growth parameters measured (**Table SIb**).

281 The taxonomy of the initial community, as well as the taxonomy of each sorted fraction (EdU^+,
282 whole community) for each treatment (Control, Polymyxin B, Vancomycin) is displayed at the
283 genus level in **Figure 4b**. When comparing the control to the Polymyxin B treatment, and
284 accounting for sorted fraction as a random effect (see Methods), differential abundance analysis

285 identified *Muribaculaceae* and *Akkermansia* as significantly decreased in the Polymyxin B
286 treatment (*Muribaculaceae*: from 39.08% ± 15.58 to 5.51% ± 7.07; *Akkermansia*: from 3.17% ±
287 2.19 to 1.31% ± 1.72). This is consistent with the expected effect of this antibiotic on Gram
288 negative bacteria. There were no differentially abundant species between the control and the
289 Vancomycin treatment.

290 Differential abundance analysis on the sorted fractions for all treatments and accounting for
291 treatment as a random effect (see Methods) revealed two differentially abundant genera:
292 *Desulfovibrio* and *Ileibacterium*.

293 *Desulfovibrio* was differentially abundant due to its exclusion from the EdU^+ group, as despite its
294 low abundance in the other fractions (Whole: 1.04% ± 0.74; Initial 0.37% ± 1.15), it was virtually
295 absent from the EdU^+ fraction (0.03% ± 0.07). This suggests either that this bacterium is not
296 actively replicating, or that it is not amenable to labeling with EdU.

297 As previously observed, *Ileibacterium* dominated the EdU^+ fraction (67.08% ± 33.27) in
298 comparison to the Whole (22.14% ± 11.07) and Initial (11.93% ± 1.14) fractions, regardless of the
299 treatment. This contrasts with the known effects of vancomycin on Gram positive bacteria.

300 The PCoA on the weighted Unifrac distances for these conditions can be seen in **Figure 4c**. The
301 EdU^+ fractions of all the treatment groups cluster together and are distinct from the rest of the
302 populations, and the EdU^+ fraction is significantly different from the whole community ($q =$
303 0.045). There was no significant difference in the weighted Unifrac distance between any of the
304 treatments ($q > 0.05$), again likely due to the significant clustering together of the EdU^+ fractions
305 from all treatment groups (**Fig. 4c**).

306 The Shannon index values for each treatment condition can be seen in **Figure 4d**. Once again, the
307 EdU^+ fractions had a significantly lower Shannon index as compared to the whole community (q
308 = 0.016) and the initial community (q = 0.037) sorted fractions, regardless of treatment type
309 (exposure or not to either antibiotic). Furthermore, the initial community had a significantly higher
310 Shannon index as compared to the whole community (q = 0.037). When considering the different
311 treatment types regardless of the sorted fraction, there were no significant differences in the
312 Shannon index values between the treatments, possibly due to the low Shannon index values in all
313 EdU^+ fractions (**Fig. 4d**).

314

315 **Discussion**

316 We describe here the optimization of EdU "click" chemistry (EdU-click) paired with FACS and
317 16S amplicon sequencing to identify replicating gut bacteria *in vitro*. We first show that EdU-click
318 labels gut bacterial isolates with no bias based on cell wall type, yet reveals notably fewer
319 Bacteroidetes labeled relative to Firmicutes (**Fig. 1d**). The results we have gathered thus far
320 suggest genus-level variation in EdU labeling, though more thorough investigations with other gut
321 bacterial isolates are needed to confirm this.

322 We note that not all gut bacterial isolates were amenable to EdU-click. As mentioned in the
323 Results, this did not seem to be due to differences in cell wall type. There was, however, a
324 significant positive correlation between the replication rate of an isolate and the proportion of its
325 cells which were labeled (**Fig. S1c**), suggesting that bacteria must grow rapidly during the
326 incubation with EdU in order to be labeled. However, replication rate alone cannot fully explain

327 the discrepancies in labeling seen here, since *B. infantis* grew rapidly (**Fig. S1b**) but did not label
328 (**Fig. S1a**).

329 Another possible explanation could be phylogenetic differences in the ability to uptake or use
330 exogenous pyrimidine nucleosides (such as thymidine, of which EdU is an analogue), which has
331 been shown to affect bacterial DNA labeling in other complex communities.[35,36] Even when
332 bacteria encode the genes to use thymidine, some may preferentially use the *de novo* pathway
333 rather than the salvage pathway to make nucleotides,[37] the latter being required for EdU labeling.
334 Further work on other gut bacterial isolates, especially members of the phyla with many unlabeled
335 representatives, is thus required to identify the underlying mechanisms.

336 Regardless of the reason for the lack of labeling of certain bacterial isolates, these results confirm
337 that EdU-click can only inform about the replication dynamics of bacteria which are both amenable
338 to labeling and which are actively replicating. This is a known problem when using thymidine
339 analogues to track replicating bacterial populations, as mentioned previously.[35,36,38]. Since the
340 ability of all environmental microorganisms to uptake thymidine analogues like EdU remains
341 undetermined, the results from EdU-click should be interpreted cautiously when used in microbial
342 assemblages.

343 Despite these inherent limitations, we optimized the EdU-click procedure for mouse fecal bacterial
344 communities, as even partial knowledge of the replicating gut bacteria could provide a more
345 nuanced understanding of gut microbial dynamics, community metabolism and, ultimately, host
346 metabolism.[15,21] Based on our experience, the EdU-click optimization process we have done here
347 should be done for any other microbial ecosystem of interest, following our framework.

348 When characterizing the EdU^+ cells derived from the feces of healthy mice, we report that the
349 EdU^+ fraction had significantly lower alpha diversity metrics, and a significantly different
350 weighted Unifrac distance, as compared to the whole community, regardless of the cage of origin.
351 These results suggest that the EdU^+ fraction is a specific subset of the whole community. This is
352 further supported by taxonomic analysis, which revealed that the EdU^+ fraction was enriched in
353 *Ileibacterium* and *Prevotella* UCG-001, and depleted in *Akkermansia* and *Dubosiella*, as compared
354 to the whole community.

355 There is not much literature on *Ileibacterium*, with only one characterized species, *I. valens*, in
356 2017.[39] So far, *I. valens* has been seen to increase in abundance after dietary changes,[39-42] and it
357 has been associated with a few immunological and host physiological parameters.[42] Our results
358 here suggest that it may be a very actively replicating member of the mouse gut microbiota, though
359 its specific roles in the gut are yet to be determined.

360 The EdU procedure developed here requires an incubation step which can still lead to an altered
361 community structure, despite our efforts to minimize this. Indeed, the diversity and taxonomic
362 composition of the initial community differed from that of the incubated whole community in all
363 experiments in this study. Namely, incubation resulted in decreased richness due to the loss of less
364 abundant taxa, either not supported by the incubation medium or lost during the click procedure
365 and sorting steps (**Fig. 3b,e; Fig. 4b,d**).

366 EdU-click may thus capture the replication potential of the more abundant gut bacterial members
367 which are amenable to labeling, rather than accurate *in situ* replication of all members present.
368 Nevertheless, replication potential has been shown to strongly correlate with *in situ* replication,[43]
369 and *in vitro* incubations of microbial communities for several hours outside their original
370 ecosystems have been shown to not alter the original *in situ* replication patterns.[33] Overall, this

371 suggests that EdU-click can still provide useful information on *in situ* dynamics for the most
372 abundant bacterial members or those with a higher growth rate, despite necessitating an *in vitro*
373 incubation step.

374 Finally, we demonstrate one potential application of our optimized EdU-click technique in an *in*
375 *vitro* antibiotic perturbation experiment on mouse fecal bacteria incubated with either polymyxin
376 B or vancomycin. Polymyxin B exposure resulted in a decrease in the relative abundance of
377 *Muribaculaceae* and *Akkermansia* (both Gram-negative bacteria), whereas vancomycin did not
378 have a large effect on the bacterial community or its Gram-positive members. Importantly,
379 *Ileibacterium* constituted the vast majority of the EdU^+ fraction in both the polymyxin B and the
380 vancomycin treatment.

381 One explanation for the replication of *Ileibacterium* during exposure to vancomycin is that this
382 taxon was replicating and incorporating EdU before the antibiotic affected its growth. This is
383 supported by the growth curve of the vancomycin-treated bacterial community, wherein the
384 bacteria were replicating at similar rates as the control community until later in the growth curve
385 (**Fig. 4a, Table SI**). We cannot rule out other possibilities, however, such as insufficient dosage
386 of the antibiotic (despite using a final concentration of 0.1 $mg.mL^{-1}$, higher than the estimated
387 vancomycin minimal inhibitory concentration [MIC] of 0.001-0.01 $mg.mL^{-1}$ for these samples;
388 data not shown) or innate resistance of *Ileibacterium* to vancomycin.

389 To investigate the latter, we identified genes in the only sequenced *I. valens* genome available
390 which were homologous to known antimicrobial resistance genes, using the Comprehensive
391 Antibiotic Resistance Database (CARD) Resistance Gene Identifier (RGI) on the translated protein
392 sequences of this genome.[39,44] The results were inconclusive, as there were only loose hits to a
393 variety of antibiotic resistance genes. These included hits to 21 vancomycin and glycopeptide

394 resistance genes (**Table SII**) as well as 69 hits to genes related to various antibiotic efflux pumps
395 (data not shown). Despite being loose hits, either strategy – glycopeptide resistance or antibiotic
396 efflux – could explain the ability of *Ileibacterium* to replicate during exposure to vancomycin.
397 Furthermore, other members of the *Erysipelotrichaceae* family, to which *Ileibacterium* belongs,
398 have been reported as being intrinsically resistant to vancomycin.[45-47] Considering that
399 mechanisms for resistance against glycopeptide antibiotics like vancomycin can differ greatly
400 between taxa and remain to be fully characterized in all bacteria,[48] it is thus still possible that
401 *Ileibacterium* is truly resistant to vancomycin.

402 Overall, we show that EdU-click enables the rapid detection of replicating bacteria, both in clonal
403 populations and in heterogenous microbial assemblages. The procedure is not laborious and it
404 gives valuable qualitative information on bacterial replication. Furthermore, complementing EdU-
405 click with cell sorting and DNA sequencing allows for the taxonomic characterization of actively
406 replicating bacteria. Coupling this information with knowledge of the taxonomic composition of
407 the overall bacterial community can help reveal differential bacterial replication strategies in
408 homeostatic and disrupted conditions, as observed in this work.

409 Our modified EdU-click procedure can best be applied for studying bacterial replication *in situ*
410 and *in vitro*, where the ability of the resident bacteria to be labeled with EdU has been determined
411 beforehand. For instance, bacterial communities known to label with EdU could be incubated with
412 EdU in their natural environment (e.g., seawater, soil slurries, activated sludge). This technique
413 would also be useful for tracking the replicating members of simplified bacterial communities in
414 artificial gut systems (e.g., intestinal organoids, bioreactors, chemostats), or when only the
415 replication of specific taxa is of interest. Furthermore, tracking replicating bacterial communities
416 over time using EdU-click will help reveal the dynamics of specific bacterial replication and their

417 impacts on the metabolism and composition of bacterial communities. This technique will be
418 especially informative for tracking changes in bacterial replication and composition during the
419 establishment of bacterial communities (e.g., in early life), during homeostasis, and as changes
420 occur in the environment of these bacteria (e.g., antibiotic administration, intestinal pathogen
421 infection).

422 Going forward, it would be worth further investigating the cause(s) of the differential labeling of
423 bacterial isolates with EdU and quantifying the amount of EdU entering the cells. Importantly,
424 uncovering the possible roles of *I. valens* in the colons of healthy mice and its apparent resistance
425 to vancomycin will also be key to better understand the resilience of certain bacterial taxa to
426 perturbations.

427

428 **Methods**

429 ***Animals***

430 Feces from male and female wild-type C57BL/6 mice (Jackson Laboratories) kept at the Goodman
431 Cancer Center at McGill University were collected, in accordance with the McGill Ethics Research
432 Board (animal ethics protocol #5287). Over the course of the EdU optimization process and *in*
433 *vitro* experiments, different cages of mice with varying ages were used. During the experiments
434 on the healthy mouse gut microbiota, mice were matched for age. In experiment 1, the mice were
435 6 weeks and 6 days old and consisted of 4 male mice and 4 female mice of the same origin. In
436 experiment 2, the mice were 7 weeks and 3 days old, and consisted of 4 male mice and 5 female
437 mice of the same origin, with the except of one female mouse which was from a different litter. It

438 should be noted that the same feces from the mice in experiment 2 were used for the antibiotic
439 perturbation experiment (see *EdU-click performed on antibiotic-treated mouse fecal bacteria*).

440 In all cases, experiments were conducted on a mixture of feces from both male and female mice.
441 Fecal pellets were collected from the mice by putting each mouse into its own cage, empty of
442 corncob bedding and nesting material, with no access to food or water. Feces from each mouse
443 were collected soon after defecation. Feces from mice of the same cage were put into the same 1.5
444 mL microcentrifuge tube. This procedure lasted no longer than one hour, after which mice were
445 placed back into their respective cages. This procedure was never repeated more than twice in one
446 week. Immediately after this collection procedure, the fecal pellets were either processed in an
447 anaerobic chamber as detailed in *Isolation of bacteria from mouse* feces or frozen at -80°C.

448 ***Bacterial strains***

449 The bacterial strains used in this study were *Bacteroides fragilis* (32-6-I 11 MRS AN), *Escherichia*
450 *coli K12 (*ATCC 25404*), Bifidobacterium longum* subsp. *infantis (*ATCC 15697*), Bacteroides*
451 *caccae (*ATCC 43185*), Prevotella intermedia (*ATCC 25611*), Clostridium beijerinckii (*ATCC
452 51743*), Ruminococcus bromii (*ATCC 27255*), Akkermansia muciniphila (*ATCC BAA-835*)*, and
453 *Enterococcus faecalis* (SF24397). Each bacterium was originally isolated from the human gut,
454 with the exception of *P. intermedia*, which comes from the human oral cavity. All bacteria were
455 cultured anaerobically in an anerobic chamber (Coy Laboratory Products; 5% H2, 20% CO2, 75%
456 N2) at 37°C overnight directly from frozen (-80°C) glycerol stocks, in autoclaved reduced Bovine
457 Heart Infusion (rBHI) broth (Oxoid).

458 ***Absorbance spectroscopy and EdU labeling of bacterial isolates***

459 Overnight cultures of bacterial isolates were diluted in rBHI in a Falcon multiwell 24-well plate
460 (Corning) to an optical density at 600 nm (OD600) of 0.05, with six replicate wells per isolate;
461 three replicates were incubated with 20 µM EdU (from the Click-iT EdU Alexa Fluor™ 647 flow
462 cytometry assay kit, ThermoFisher Scientific) and three replicates were not incubated with EdU.
463 For those replicates incubated without EdU, an equivalent volume of reduced 1X 0.2 µm-filtered
464 phosphate-buffered saline (rPBS – 1 mg mL−1 L-cysteine) (Bioshop) was added to each well. For
465 *E. faecalis* and *E. coli* K12, only two wells were used for the microscopy and replication
466 measurements - one incubated with EdU, and one without. Additionally, *R. bromii* had two wells
467 incubated with EdU and two without, due to the limited growth of the overnight culture.

468 All bacteria were incubated anaerobically in the 24-well plate at 37°C for 3 hours in an Epoch 2
469 Microplate Spectrophotometer (BioTek), with optical density measured at 600 nm (OD600). Every
470 15 minutes, the spectrophotometer shook the plate in a double-orbital fashion for 10 seconds and
471 read the absorbance of each well. After the incubation, the bacteria were immediately fixed in an
472 equal volume of 80% ethanol, for a final concentration of 40% ethanol. Fixed bacteria were either
473 stored at 4°C overnight or processed after 10 minutes of incubation in the ethanol. The same or the
474 next day, bacterial isolates underwent the click reaction as described in *Click reaction for bacterial*
475 *isolates and fecal-derived bacteria*, and were either observed using flow cytometry as described
476 in *Nucleic acid staining, flow cytometry, and fluorescence-activated cell sorting* or were prepared
477 for microscopy as described in *Fluorescence microscopy of bacterial isolates*.

478 ***Click reaction for bacterial isolates and fecal-derived bacteria***

479 The following procedure is the optimized version of the EdU-click method. For both bacterial
480 isolates and fecal-derived bacteria, fixed bacteria were pelleted by centrifugation (8,000xg, 5 min)
481 and washed in 1X 0.2 µm-filtered phosphate-buffered saline (PBS) (Bioshop) before undergoing

482 the click reaction as described by the kit protocol, with the exception that a final concentration of
483 5 μM of the Alexa Fluor™ 647 azide fluorophore (purchased separately as Alexa Fluor™ 647
484 azide, Triethylammonium Salt from ThermoFisher Scientific) was used. Afterwards, the bacteria
485 were again pelleted by centrifugation (8,000xg, 5 min) and washed in an equal volume of 80%
486 ethanol (final concentration 40%). The bacteria were resuspended in the diluted ethanol using filter
487 pipettes, then they were centrifuged once more (8,000xg, 5 min), the ethanol was removed, and
488 the pellet was resuspended in PBS for subsequent visualization using flow cytometry or
489 fluorescence microscopy.

490 ***Nucleic acid staining, flow cytometry, and fluorescence-activated cell sorting***

491 After the EdU-click procedure, bacterial cells were diluted as needed (between 1:100 and 1:200)
492 in PBS in 5 mL polystyrene round-bottom tubes (Falcon). All samples were stained with 1X Sybr
493 Green I nucleic acid gel stain (Sybr Green I; Invitrogen by Thermo Fisher Scientific) for 15
494 minutes before acquisition on a flow cytometer. Flow cytometric measurements were obtained
495 using the FACS Canto II (BD Biosciences, San Jose, CA, USA) equipped with a solid-state blue
496 laser (488 nm, 20-mW) and a He/Ne ion red laser (633-nm, 17-mW) with BD FACSDiva software
497 (BD Biosciences). The blue laser was used to excite Sybr Green I, and the green-fluorescence
498 emission from Sybr Green was collected in the FITC channel (BP 530/30 filter). The red laser was
499 used to excite the Alexa Fluor™ 647 fluorophore, and the red-fluorescence emission from this
500 fluorophore was collected in the APC channel (BP 660/20). Forward angle light scatter (FSC) was
501 collected in the FSC channel, and side angle light scatter (SSC) was collected in the SSC channel
502 (BP 488/10 filter).

503 When the bacterial cells underwent fluorescence-activated cell sorting (FACS), the FACSAria II
504 (BD Biosciences, San Jose, CA, USA) was used, which is equipped with a solid-state blue laser

505 (488 nm, 20-mW) and a He/Ne ion red laser (633-nm, 17-mW) with BD FACSDiva software (BD
506 Biosciences). The same excitation and emission parameters as used during flow cytometry were
507 also used for cell sorting.

508 Data obtained from flow cytometry and FACS were analyzed using FlowJo™ software. Cell
509 numbers were calculated from flow cytometry data using standards of known size and number.
510 EdU+ cells were classified as those events which appeared in the upper right section of the flow
511 cytogram (Q2). EdU- cells were classified as those events which appeared in the lower right section
512 of the flow cytogram (Q3) when the sample was incubated with EdU. Any events which appeared
513 in Q2 when the sample was incubated without EdU were classified as noise and subtracted from
514 the number of EdU+ cells. The proportions of EdU+ cells were quantified as the number of cells
515 in Q2 minus the average amount of noise and divided by the sum of cells present in Q2 and Q3.

516 ***Fluorescence microscopy of bacterial isolates***

517 After undergoing the click reaction as described in *Click reaction for bacterial isolates and fecal-*
518 *derived bacteria*, bacterial isolates were prepared for microscopy in the following way. Bacterial
519 isolates suspended in PBS were further diluted in PBS as necessary, and then portioned into 1 mL
520 aliquots. These aliquots were stained with 1X Sybr Green I nucleic acid gel stain (Sybr Green I;
521 Invitrogen by Thermo Fisher Scientific) for 15 minutes, and then these aliquots were vacuum
522 filtered through 0.22 um filters on top of 0.3 um filters. Once the filters were dry, they were placed
523 onto a microscope slide that had a drop of Citifluor AF1 Mountant Solution (Electron Microscopy
524 Sciences) on it. A coverslip treated with this same antifade was then placed on top of the filter.
525 The coverslip was sealed onto the microscope slide using commercially available nail polish. Once
526 the slides were sealed, they were stored at -20°C until they were visualized.

527 Visualization of slides typically occurred the day after the slides were prepared, but never later
528 than 1 week after slide preparation. All slides were visualized using the Axiovert 3 widefield
529 inverted microscope (Zeiss) equipped with a Zeiss Axiocam 506 monochrome CCD camera (2752
530 x 2208 pixels, 4.54 um pixels) and Sola SM solid state light engine, using the 100X objective
531 (PLAN-APOCHROMAT, NA=1.4, OIL, Iris) under oil immersion and the FS 24 (FITC) and FS
532 32 (Cy5) fluorescence cubes. Images were further processed in Fiji (version 1.53q).

533 ***Isolation of bacteria from mouse feces***

534 Fresh fecal pellets were collected in 1.5 mL microcentrifuge tubes from wildtype C57BL/6 mice
535 on the day of EdU incubation. Fecal pellets were diluted as 1 µg of feces in 10 µl liquid (1:10) in
536 1.5 mL microcentrifuge tubes using reduced 1X 0.2 µm-filtered phosphate-buffered saline (rPBS
537 – 1 mg mL−1 L-cysteine) (Bioshop) and vortexed thoroughly until no solid pellet remained (~2-5
538 minutes). The tubes were then centrifuged for 1 minute at 700xg, and the supernatant was removed
539 and added to a new 1.5 mL tube. These new tubes were centrifuged for 3 minutes at 6,000xg, and
540 the resulting supernatant from all tubes was added into one 15 mL centrifuge tube. This
541 supernatant, called the "fecal slurry", was saved as part of the medium in which the bacteria would
542 be incubated. The pellet was then resuspended in rPBS and centrifuged again, for 2 minutes at
543 6,000xg. The supernatant was discarded and the pellet was resuspended once more in rPBS. The
544 resulting mixture was used as fecal-derived bacterial cells.

545 ***EdU labeling of fecal-derived bacteria***

546 The following procedure is the optimized version of the EdU-click method; note that the
547 incubation medium, EdU concentration, and incubation time were different during optimization
548 (see Results). Fecal-derived bacteria were diluted 1:10 in a medium made of 50% rBHI and 50%

549 fecal slurry (1:1 rB/FS). These bacteria were incubated anaerobically at 37°C for 3 hours in 1.5
550 mL microcentrifuge tubes in triplicate or duplicate with or without a final concentration of 20 μM
551 EdU, respectively. Immediately after the incubation, bacterial cells were fixed in an equal volume
552 of 80% ethanol (final concentration 40%) and stored at 4°C overnight. The next day, fecal-derived
553 bacteria underwent the click reaction and were observed using flow cytometry as described in
554 *Click reaction for bacterial isolates and fecal-derived bacteria* and *Nucleic acid staining, flow*
555 *cytometry and fluorescence-activated cell sorting*, respectively.

556 ***EdU-click performed on feces of healthy mice***

557 Fecal-derived bacteria were isolated from two cages of mice (one male cage, one female cage), as
558 described under *Animals*, in two independent experiments. In each experiment, feces from each
559 cage were pooled into their own 1.5 mL tube. EdU-click was performed as described in *EdU*
560 *labeling of fecal-derived bacteria*, except that in each experiment, the bacteria were first incubated
561 in 3 wells of a 96-well plate for 1 hour in an Epoch 2 Microplate Spectrophotometer (BioTek),
562 with optical density measured at 600 nm (OD600). Every 15 minutes, the spectrophotometer shook
563 the plate in a double-orbital fashion for 10 seconds and read the absorbance of each well. After
564 this 1-hour incubation, 2 μl of DMSO was added to the culture in addition to 20 μM (final
565 concentration) of EdU or an equal volume of rPBS, where appropriate, and the plate was incubated
566 for another 3 hours in the spectrophotometer, after which the bacteria were fixed and stored as
567 described in *EdU labeling of fecal-derived bacteria*.

568 After the click reaction and nucleic acid staining were performed as described in *Click reaction*
569 *for bacterial isolates and fecal-derived bacteria*, bacterial cells underwent cell sorting as described
570 in *Nucleic acid staining, flow cytometry and fluorescence-activated cell sorting*. The following
571 populations were sorted: (1) Whole, unincubated community (initial community); (2) EdU+ cells;

572 (3) EdU- cells; and (4) Whole, incubated community. Populations (1) and (4) were sorted based
573 on their Sybr Green I nucleic acid signal, whereas populations (2) and (3) were sorted from each
574 other based on their Alexa Fluor™ 647 signal (for EdU incorporation).

575 ***Antibiotics***

576 The antibiotics used in this study were vancomycin (vancomycin hydrochloride from *Streptomyces*
577 *orientalis*, Sigma Life Sciences lot # 085M4163V) and polymyxin B (polymyxin B sulfate,
578 BioShop lot # 4F34412). Both were dissolved in 100% dimethyl sulfoxide (DMSO) to a
579 concentration of 10 mg/mL and stored at 4°C protected from light. Dilutions of this stock were
580 made and added to fecal-derived bacterial cultures at the appropriate time (see *EdU-click*
581 *performed on antibiotic-treated mouse fecal bacteria*). The final concentration of both antibiotics
582 was 1 µg/mL. This concentration was chosen based on our assessment of the minimum inhibitory
583 concentration (MIC) for these antibiotics in the specific media we used (data not shown).

584 ***EdU-click performed on antibiotic-treated mouse fecal bacteria***

585 Bacteria were extracted from fresh mouse fecal pellets obtained from healthy, wildtype C57BL/6
586 mice (see *Animals*) as described under *Isolation of bacteria from mouse feces*. These bacteria were
587 incubated anaerobically in an Epoch 2 Microplate Spectrophotometer (BioTek) at a 1:10 ratio in a
588 final culture volume of 200 µl per well in 12 wells of a 96-well plate for 1 hour in 1:1 rBHI:fecal
589 slurry. Every 15 minutes, the spectrophotometer shook the plate in a double-orbital fashion for 10
590 seconds and read the optical density of each well at 600 nm (OD600).

591 After this 1-hour incubation, the appropriate concentration of vancomycin, polymyxin B, or
592 DMSO (the vehicle), was added to the culture in addition to 20 µM (final concentration) of EdU
593 or an equivalent volume of rPBS, where appropriate. Each treatment – being vancomycin with

594 EdU, polymyxin B with EdU, DMSO with EdU, and DMSO without EdU – had 3 wells dedicated
595 to it (i.e., each treatment was performed in triplicate). After administration of the antibiotics, the
596 plate was incubated for an additional 3 hours in the same conditions as the 1-hour incubation, after
597 which the bacteria were fixed in an equal volume of 80% ethanol (final concentration 40% ethanol)
598 and stored overnight at 4°C. The following day, the click procedure was performed on these
599 samples as described under *Click reaction for bacterial isolates and fecal-derived bacteria*. The
600 EdU+ and EdU- bacteria, as well as the initial and whole community, were then sorted from these
601 samples using FACS, as described under *Nucleic acid staining, flow cytometry and fluorescence-*
602 *activated cell sorting*. DNA extraction and 16S rRNA gene sequencing were performed on these
603 populations as described under *DNA extraction from fecal-derived bacterial cells* and *16S rRNA*
604 *amplicon sequencing and analysis*.

605 ***DNA extraction from mouse fecal-derived bacterial cells***

606 Bacterial DNA was extracted from sorted and unsorted mouse fecal-derived bacterial cells using
607 the AllPrep PowerFecal DNA/RNA kit (Qiagen) as per manufacturer instructions, with the
608 following alterations: 200 µl of sorted bacterial cells were used instead of 200 mg stool, all cold
609 incubations were conducted in an ice bucket instead of at 4°C, the amount of supernatant and
610 buffer C4 used after IRS incubation was doubled, the extracted DNA was diluted in RNAse free
611 water rather than EB buffer, and the RNA collection steps were not performed. For the cell lysis
612 step, bead-beating was performed using a Vortex Genie 2 with a microtube holder (SI-H524)
613 (Scientific Industries) for 10 minutes when extracting <10 samples at a time, or for 20 minutes
614 when extracting >10 samples at a time. All extracted DNA was immediately stored at -20°C.

615 ***16S rRNA gene amplicon sequencing and analysis***

616 For both the experiment on the feces of healthy mice and the antibiotic *in vitro* perturbation
617 experiment, extracted DNA underwent library preparation and 16S rRNA gene sequencing of the
618 V4-V5 hypervariable region using the Illumina MiSeq PE250 system at the Université de Québec
619 à Montréal (UQAM) Center of Excellence in Research on Orphan Diseases – Foundation Courtois
620 (CERMO-FC) genomics platform.

621 The resulting bacterial sequences were analyzed using QIIME2 version 2022.2.[49] As described in
622 the Results, any sequences present in the sheath fluid but absent in the initial unsorted community
623 were identified and manually removed from the analysis. Briefly, we used DADA2 in QIIME2 for
624 quality control and filtering. Sequences were rarefied to a depth of 4458 reads for the healthy mice
625 and 4702 reads for the antibiotic experiment before alpha and beta diversity analyses. Specifically,
626 we used Shannon's and Simpson's indices for alpha diversity, and weighted Unifrac for beta
627 diversity. Principal component analysis (PCoA) plots were constructed using weighted Unifrac
628 distances. Significance between alpha diversity measures based on metadata (e.g., treatments,
629 cages, sex, etc.) was measured using a Kruskal-Wallace test with pairwise comparisons.
630 Significance between beta diversity measures was conducted using pairwise PERMANOVA
631 comparisons with 999 permutations.

632 Taxonomic classification and relative abundance measurements were conducted on the quality-
633 controlled, filtered sequences using QIIME2's machine-learning program pre-trained on the 16S
634 V4-V5 regions, using the Silva database.

635 Differential abundance analyses for all experiments were carried out in R (version 4.1.3) with
636 ANCOM-II with Benjamini-Hochberg correction for multiple comparisons.[50]

637 ***Statistical analyses***

638 All statistical tests outside of those conducted in QIIME2 were conducted using Prism version
639 9.3.1 (GraphPad). Results were determined to be significantly different at P-value $\leq$ 0.05.
640 Significance testing was conducted using the Kruskal-Wallis test with Dunn's multiple
641 comparisons test, Brown-Forsythe and Welch ANOVA with Dunnett's multiple comparisons test,
642 or one-way ANOVA with Dunnett's test, as described in the Figure legends.

643 Correlation analyses between bacterial isolate maximal replication rates and their respective
644 proportions of EdU+ cells were conducted by calculating Pearson's correlation coefficients in
645 Prism. Area under the curve (AUC) calculations of all bacterial growth curves was also calculated
646 in Prism.

647 **Data Availability Statement**

648 Bacterial 16S rRNA gene sequencing data can be accessed on the NCBI SRA database, accession
649 number PRJNA855973. Code related to the analysis has been deposited in GitHub
650 (https://github.com/evetb). Raw microscopy and flow cytometry data have been deposited in
651 FigShare (https://doi.org/10.6084/m9.figshare.c.6103014.v1).

652 **Disclosure of interest**

653 The authors report there are no competing interests to declare.

654 **Authors' contributions**

655 ETB designed, performed, analyzed, and interpreted experiments. CH helped with the bacterial
656 isolate experiments. CFM helped develop the project, obtained funding, helped design
657 experiments, and interpret the data. ETB and CFM edited the manuscript and approved the final
658 draft.

659 **Funding**

660 This work was supported by a Frederick Banting and Charles Best Canada Graduate Scholarship-
661 Master's (CGS M) award and a Ferrings Pharmaceuticals Fellowship to ETB. This work was also
662 supported by the Canada Research Chair program (950-230748 X-242502), an Innovator Award
663 to CFM from the Kenneth Rainin Foundation (2016-1280), and the McGill University Health
664 Centre Foundation (Owen Catchpaugh IBD research grant). CFM is a Tier 2 Canada Research
665 Chair in Gut Microbiome physiology.

666 **Acknowledgements**

667 The authors would like to thank all the members of the Maurice lab, as well as Professor Bastien
668 Castagner and Professor Gregory Marczynski, for their help editing parts of this manuscript. The
669 flow cytometry work was performed in the McGill University Flow Cytometry Core Facility for
670 flow cytometry and single cell analysis of the Life Science Complex and supported by funding
671 from the Canadian Foundation for Innovation. The microscopy was performed in the McGill
672 University Advance Bioimaging Facility (ABIF), RRID:SCR_017697.

673 **References**

674 1. Li J, Butcher J, Mack D, et al. Functional impacts of the intestinal microbiome in the
675 pathogenesis of inflammatory bowel disease. *Inflamm Bowel Dis*. 2015 Jan;21(1):139-53.
676 2. Lloyd-Price J, Abu-Ali G, Huttenhower C. The healthy human microbiome. *Genome Med*.
677 2016 Apr 27;8(1):51.
678 3. Mirzaei MK, Maurice CF. Menage a trois in the human gut: interactions between host,
679 bacteria and phages. *Nat Rev Microbiol*. 2017 Jul;15(7):397-408.

680 4. Shkoporov AN, Hill C. Bacteriophages of the Human Gut: The "Known Unknown" of the
681 Microbiome. *Cell Host Microbe*. 2019 Feb 13;25(2):195-209.
682 5. Gill SR, Pop M, Deboy RT, et al. Metagenomic analysis of the human distal gut
683 microbiome. *Science*. 2006 Jun 2;312(5778):1355-9.
684 6. Lozupone CA, Stombaugh JI, Gordon JI, et al. Diversity, stability and resilience of the
685 human gut microbiota. *Nature*. 2012 Sep 13;489(7415):220-30.
686 7. Schirmer M, Garner A, Vlamakis H, et al. Microbial genes and pathways in inflammatory
687 bowel disease. *Nat Rev Microbiol*. 2019 Aug;17(8):497-511.
688 8. Franzosa EA, Morgan XC, Segata N, et al. Relating the metatranscriptome and
689 metagenome of the human gut. *Proc Natl Acad Sci U S A*. 2014 Jun 3;111(22):E2329-38.
690 9. Franzosa EA, Sirota-Madi A, Avila-Pacheco J, et al. Gut microbiome structure and
691 metabolic activity in inflammatory bowel disease. *Nat Microbiol*. 2019 Feb;4(2):293-305.
692 10. Qin J, Li R, Raes J, et al. A human gut microbial gene catalogue established by
693 metagenomic sequencing. *Nature*. 2010 Mar 4;464(7285):59-65.
694 11. Schirmer M, Franzosa EA, Lloyd-Price J, et al. Dynamics of metatranscription in the
695 inflammatory bowel disease gut microbiome. *Nat Microbiol*. 2018 Mar;3(3):337-346.
696 12. Tropini C, Earle KA, Huang KC, et al. The Gut Microbiome: Connecting Spatial
697 Organization to Function. *Cell Host Microbe*. 2017 Apr 12;21(4):433-442.
698 13. Moen AEF, Lindstrom JC, Tannaes TM, et al. The prevalence and transcriptional activity
699 of the mucosal microbiota of ulcerative colitis patients. *Sci Rep*. 2018 Nov 22;8(1):17278.
700 14. Hatzenpichler R, Krukenberg V, Spietz RL, et al. Next-generation physiology approaches
701 to study microbiome function at single cell level. *Nat Rev Microbiol*. 2020 Apr;18(4):241-
702 256.

703 15. Brown CT, Olm MR, Thomas BC, et al. Measurement of bacterial replication rates in
704 microbial communities. *Nat Biotechnol*. 2016 Dec;34(12):1256-1263.
705 16. Koch BJ, McHugh TA, Hayer M, et al. Estimating taxon-specific population dynamics in
706 diverse microbial communities. *Ecosphere*. 2018;9(1):e02090.
707 17. Long AM, Hou S, Ignacio-Espinoza JC, et al. Benchmarking microbial growth rate
708 predictions from metagenomes. *ISME J*. 2021 Jan;15(1):183-195.
709 18. Myhrvold C, Kotula JW, Hicks WM, et al. A distributed cell division counter reveals
710 growth dynamics in the gut microbiota. *Nat Commun*. 2015 Nov 30;6:10039.
711 19. Riglar DT, Richmond DL, Potvin-Trottier L, et al. Bacterial variability in the mammalian
712 gut captured by a single-cell synthetic oscillator. *Nat Commun*. 2019 Oct 11;10(1):4665.
713 20. Joseph TA, Chlenski P, Litman A, et al. Accurate and robust inference of microbial growth
714 dynamics from metagenomic sequencing reveals personalized growth rates. *Genome Res*.
715 2022 Mar;32(3):558-568.
716 21. Korem T, Zeevi D, Suez J, et al. Growth dynamics of gut microbiota in health and disease
717 inferred from single metagenomic samples. *Science*. 2015 Sep 4;349(6252):1101-1106.
718 22. Hudak JE, Alvarez D, Skelly A, et al. Illuminating vital surface molecules of symbionts in
719 health and disease. *Nat Microbiol*. 2017 Jun 26;2:17099.
720 23. Kuru E, Hughes HV, Brown PJ, et al. In Situ probing of newly synthesized peptidoglycan
721 in live bacteria with fluorescent D-amino acids. *Angew Chem Int Ed Engl*. 2012 Dec
722 7;51(50):12519-23.
723 24. Lin L, Wu Q, Song J, et al. Revealing the in vivo growth and division patterns of mouse
724 gut bacteria. *Sci Adv*. 2020 Sep;6(36).

725 25. Wang W, Lin L, Du Y, et al. Assessing the viability of transplanted gut microbiota by
726 sequential tagging with D-amino acid-based metabolic probes. *Nat Commun*. 2019 Mar
727 21;10(1):1317.
728 26. Taguer M, Shapiro BJ, Maurice CF. Translational activity is uncoupled from nucleic acid
729 content in bacterial cells of the human gut microbiota. *Gut Microbes*. 2021 Jan-
730 Dec;13(1):1-15.
731 27. Salic A, Mitchison TJ. A chemical method for fast and sensitive detection of DNA
732 synthesis in vivo. *Proc Natl Acad Sci U S A*. 2008 Feb 19;105(7):2415-20.
733 28. Steward GF, Azam F. Bromodeoxyuridine as an alternative to 3H-thymidine for measuring
734 bacterial productivity in aquatic samples. *Aquatic Microbial Ecology*. 1999;19:57-66.
735 29. Smriga S, Samo T, Malfatti F, et al. Individual cell DNA synthesis within natural marine
736 bacterial assemblages as detected by 'click' chemistry. *Aquatic Microbial Ecology*. 2014
737 07/10;72:269-280.
738 30. Kurm V, van der Putten WH, de Boer W, et al. Low abundant soil bacteria can be
739 metabolically versatile and fast growing. *Ecology*. 2017;98(2):555-564.
740 31. Ferullo DJ, Cooper DL, Moore HR, et al. Cell cycle synchronization of Escherichia coli
741 using the stringent response, with fluorescence labeling assays for DNA content and
742 replication. *Methods*. 2009 May;48(1):8-13.
743 32. Spahn C, Endesfelder U, Heilemann M. Super-resolution imaging of Escherichia coli
744 nucleoids reveals highly structured and asymmetric segregation during fast growth. *J Struct*
745 *Biol*. 2014 Mar;185(3):243-9.
746 33. Rousk J, Baath E. Growth of saprotrophic fungi and bacteria in soil. *FEMS Microbiol Ecol*.
747 2011 Oct;78(1):17-30.

748 34. Singh G, Brass A, Cruickshank SM, et al. Cage and maternal effects on the bacterial
749 communities of the murine gut. *Sci Rep*. 2021 May 10;11(1):9841.
750 35. Jeffrey WH, Paul JH. Thymidine uptake, thymidine incorporation, and thymidine kinase
751 activity in marine bacterium isolates. *Appl Environ Microbiol*. 1990;56(5):1367-1372.
752 36. Pérez MT, Hörtnagl P, Sommaruga R. Contrasting ability to take up leucine and thymidine
753 among freshwater bacterial groups: implications for bacterial production measurements.
754 *Environmental Microbiology*. 2010;12(1):74-82.
755 37. Pedrós-Alió C, Newell SY. Microautoradiography study of thymidine uptake in brackish
756 waters around Sapelo Island, Georgia, USA. *Marine Ecology-progress Series - MAR*
757 *ECOL-PROGR SER*. 1989 07/06;55:83-94.
758 38. Tsuchiya K, Sano T, Tomioka N, et al. Incorporation characteristics of exogenous 15N-
759 labeled thymidine, deoxyadenosine, deoxyguanosine and deoxycytidine into bacterial
760 DNA. *PLOS ONE*. 2020;15(2):e0229740.
761 39. Cox LM, Sohn J, Tyrrell KL, et al. Description of two novel members of the family
762 Erysipelotrichaceae: Ileibacterium valens gen. nov., sp. nov. and Dubosiella newyorkensis,
763 gen. nov., sp. nov., from the murine intestine, and emendation to the description of
764 Faecalibaculum rodentium. *Int J Syst Evol Microbiol*. 2017 May;67(5):1247-1254.
765 40. Bhat SF, Pinney SE, Kennedy KM, et al. Exposure to high fructose corn syrup during
766 adolescence in the mouse alters hepatic metabolism and the microbiome in a sex-specific
767 manner. *J Physiol*. 2021 Mar;599(5):1487-1511.
768 41. den Hartigh LJ, Gao Z, Goodspeed L, et al. Obese Mice Losing Weight Due to trans-10,cis-
769 12 Conjugated Linoleic Acid Supplementation or Food Restriction Harbor Distinct Gut
770 Microbiota. *J Nutr*. 2018 Apr 1;148(4):562-572.

771 42. Xia F, Xiang S, Chen Z, et al. The probiotic effects of AB23A on high-fat-diet-induced
772 non-alcoholic fatty liver disease in mice may be associated with suppressing the serum
773 levels of lipopolysaccharides and branched-chain amino acids. *Arch Biochem Biophys*.
774 2021 Dec 15;714:109080.
775 43. Weissman JL, Hou S, Fuhrman JA. Estimating maximal microbial growth rates from
776 cultures, metagenomes, and single cells via codon usage patterns. *Proc Natl Acad Sci U S*
777 *A*. 2021 Mar 23;118(12).
778 44. Alcock BP, Raphenya AR, Lau TTY, et al. CARD 2020: antibiotic resistome surveillance
779 with the comprehensive antibiotic resistance database. *Nucleic Acids Res*. 2020 Jan
780 8;48(D1):D517-D525.
781 45. Kwok AHY, Li Y, Jiang J, et al. Complete genome assembly and characterization of an
782 outbreak strain of the causative agent of swine erysipelas--Erysipelothrix rhusiopathiae
783 SY1027. *BMC Microbiol*. 2014;14:176-176.
784 46. Romney M, Cheung S, Montessori V. Erysipelothrix rhusiopathiae endocarditis and
785 presumed osteomyelitis. *Can J Infect Dis*. 2001 Jul;12(4):254-6.
786 47. Wu J, Liu M, Zhou M, et al. Isolation and genomic characterization of five novel strains
787 of Erysipelotrichaceae from commercial pigs. *BMC Microbiol*. 2021 Apr 23;21(1):125.
788 48. Klein G, Hallmann C, Casas IA, et al. Exclusion of vanA, vanB and vanC type glycopeptide
789 resistance in strains of Lactobacillus reuteri and Lactobacillus rhamnosus used as
790 probiotics by polymerase chain reaction and hybridization methods. *J Appl Microbiol*.
791 2000 Nov;89(5):815-24.
792 49. Bolyen E, Rideout JR, Dillon MR, et al. Reproducible, interactive, scalable and extensible
793 microbiome data science using QIIME 2. *Nat Biotechnol*. 2019 Aug;37(8):852-857.

794 50. Kaul A, Mandal S, Davidov O, et al. Analysis of Microbiome Data in the Presence of
795 Excess Zeros. *Front Microbiol*. 2017;8:2114.

796

797 **Figure Legends**

798 ***Figure 1. Optimization of EdU-click in gut bacterial isolates***. Gut bacterial isolates underwent
799 the EdU-click procedure as described in the main text. (A) Overview of the EdU-click and FACS-
800 Seq procedure. In Step 1, bacterial cells are incubated *in vitro* with EdU. In Step 2, the alkyne
801 group of the EdU molecule, located within the bacterial DNA, is exposed to a fluorescent azide
802 and undergoes a copper-catalyzed 'click' reaction. In Step 3, bacteria which have incorporated
803 EdU become fluorescent, are detected, and physically separated from unlabeled bacteria. In Step
804 4, bacterial DNA from both labeled and unlabeled bacteria undergo 16S amplicon sequencing and
805 taxonomic analysis. (B) Top: Representative flow cytograms of *Enterococcus faecalis* grown
806 either with or without EdU. Isolates grown without EdU were used to setup the gating strategy and
807 determine background noise or unspecific labeling. Quadrant 3 (Q3): unlabeled, or EdU-negative
808 (EdU-), population. Quadrant 2 (Q2): EdU+ population. Bottom: epifluorescence microscopy
809 images of the same isolate in the flow cytograms above. Scale bar: 10 microns. (C) Top:
810 Representative flow cytograms of *Bacteroides caccae* grown either with or without EdU. Bottom:
811 epifluorescence microscopy images of the same isolate in the flow cytograms above. Scale bar: 10
812 microns. (D) Quantification of the proportion of EdU+ cells for each bacterial isolate. The
813 proportion of EdU+ cells for each isolate was calculated as the average number of cells present in
814 Q2, minus background noise, divided by the sum of cells in Q2 and Q3.

815 ***Fig. 2. Optimization of EdU-click in fecal mouse bacteria***. Mouse fecal bacteria underwent
816 variations of the EdU-click procedure as described in the main text. (A) The proportion of fecal
817 bacterial cells labeled as EdU+ using increasing concentrations of EdU. (B) The proportion of
818 fecal bacterial cells labeled as EdU+ when using various combinations of media (rBHI) and fecal
819 slurry. Comparisons are relative to 100% rBHI. Statistical significance determined by Kruskal-
820 Wallis with Dunn's test to correct for multiple comparisons. Comparisons are considered
821 significant at $p \leq 0.05$. rBHI = reduced Bovine Heart Infusion broth with hemin; FS = fecal slurry;
822 rB/FS = rBHI and fecal slurry. (C) Left: The number of fecal bacterial cells, as calculated from the
823 events during flow cytometry, after each incubation time. Statistical significance determined using
824 Kruskal-Wallis with multiple comparisons corrected by Dunn's test. Initial = no incubation; o/n=
825 overnight (19 hours). Right: The proportion of fecal bacterial cells labeled as EdU+ after each
826 incubation time. Statistical significance determined using Brown-Forsythe and Welch ANOVA
827 with Dunnett's multiple comparisons test Different letters denote a significant difference at $p \leq$
828 0.05. (D) Representative flow cytogram of a mouse fecal bacterial community which underwent
829 the optimized EdU-click procedure, incubated with or without EdU.

830 ***Fig. 3. Taxonomy and diversity of fecal mouse bacteria after EdU-click***. Mouse fecal bacteria
831 from C57BL/6 mice (N= 4-5/ experiment) underwent the optimized EdU-click procedure and were
832 subsequently sorted by fluorescence and analyzed by 16S amplicon sequencing. (A) The relative
833 abundance of fecal bacteria for each experiment and each sorted fraction (initial and whole
834 community, EdU+, and EdU- cells) at the genus level. The names of bacteria which are
835 differentially abundant between the sorted fractions are bolded. (B) Principal coordinate analysis
836 (PCoA) plot of weighted UniFrac distances for each sorted fraction in (A). The different shapes
837 correspond to the two independent experiments. For the initial community, the larger point

838 corresponds to the unsorted sample whereas the smaller point corresponds to the sorted sample.
839 (C) Within-sample alpha diversity calculated using Shannon's index (i), Simpson Evenness (ii),
840 and Observed Features (iii) for each sorted fraction, combining the results from both independent
841 experiments (N=17). Initial = initial community; Whole = whole community

842 ***Fig. 4. Identifying the replicating bacterial community during an in vitro antibiotic***
843 ***perturbation.*** Mouse fecal bacteria from two different pairs of cages (n = 4-5 mice per cage) were
844 incubated in triplicate with polymyxin B, vancomycin, or no antibiotic (with DMSO, the drug
845 solvent), as well as with or without EdU. The resulting communities underwent EdU-click, cell
846 sorting, and 16S amplicon sequencing. (A) Growth curve of the fecal bacteria after addition of the
847 antibiotic or solvent, where appropriate. (B) Taxonomic composition of the initial and whole
848 community, and the EdU+ cells, for each treatment group at the genus level. Both the names of
849 the phylum and genus are provided as Phylum: Genus. Gram + bacteria are colored in shades of
850 red and pink whereas gram - bacteria are colored in shades of blue, green, orange, and purple. The
851 names of bacteria which are differentially abundant are bolded. Bacteria which were differentially
852 abundant between the different treatments have an asterisk (*) next to their names, whereas
853 differentially abundant bacteria between the sorted fractions do not. (C) Between-group beta
854 diversity (weighted UniFrac), colored by sorted fraction and with different shapes for each
855 treatment group. For the initial community (squares), the larger point corresponds to the unsorted
856 sample whereas the smaller point corresponds to the sorted sample. (D) Left: Within-group alpha
857 diversity (Shannon's index) of each sorted fraction, regardless of treatment. Right: Within-group
858 alpha diversity (Shannon's Index) of each treatment group, regardless of sorted fraction.
859 Differences in alpha diversity were determined by pairwise PERMANOVA. Significance is
860 denoted as $q \leq 0.05$. PmB = polymyxin B; Van = vancomycin.

861 ***Figure S1. Variable labelling and growth of gut bacterial isolates with EdU.*** Gut bacterial
862 isolates underwent a click reaction after incubation with 20 μM EdU, as described in the methods.
863 (A) Representative flow cytograms of each isolate grown either with or without EdU. Isolates
864 grown without EdU were used to setup our gating strategy. The horizontal line marks the top of
865 the fluorescent population in the sample grown without EdU. The vertical line separates bacterial
866 cells on the right and debris on the left. As such, everything below the horizontal line and to the
867 right (Quadrant 3; Q3) represents the unlabeled, or EdU-negative (EdU-), population, whereas
868 anything above it and to the right (Quadrant 2; Q2) represents the EdU+ population (B) Growth
869 curves of all isolates shown in (A) during incubation with EdU. (C-D). Growth rates for each of
870 the (C) nine or (D) eight (excluding *B. infantis*) bacterial isolates were calculated as the steepest
871 slope of their exponential growth curve (Max V) and were correlated with percent of cells labeled
872 with EdU (Pearson correlation). *B. longum = Bifidobacterium longum* subspecies *infantis; B.*
873 *caccae = Bacteroides caccae; B. fragilis = Bacteroides fragilis; P. intermedia = Prevotella*
874 *intermedia; C. beijerinckii = Clostridium beijerinckii; E. faecalis = Enterococcus faecalis; R.*
875 *bromii = Ruminococcus bromii; E. coli = Escherichia coli; A. muciniphila = Akkermansia*
876 *muciniphila.*

877 ***Figure S2. Heat-killed* Escherichia coli *cells do not label with EdU***. *Escherichia coli* K12
878 cultures which were either heat-killed (HK; 65°C for 1 hour) or live underwent anaerobic
879 incubation with 0 or 100 uM EdU for 2 hours, followed by the click procedure as described in the
880 main text. (A) Representative flow cytograms of Escherichia coli K12 cultures which were either
881 heat-killed (Top panel) or not (Bottom panel) before undergoing EdU-click. (B) Quantified
882 proportion of EdU+ cells, heat-killed (HK) or live, after undergoing EdU-click (C) Growth curves
883 of all conditions in (A).

884 ***Figure S3. Epifluorescence microscopy of gut bacterial isolates after EdU-click***. Human gut
885 bacterial isolates which underwent EdU-click with or without EdU were stained with Sybr Green
886 I nucleic acid dye and visualized using epifluorescence microscopy. Green = Sybr Green I, staining
887 all bacterial nucleic acid content; Red = Alexa Fluor 647 azide, staining only newly replicated
888 bacterial DNA. Any red signal seen in samples incubated without EdU was considered background
889 noise, since these signals did not correspond to the location of bacterial cells as determined by
890 Sybr Green I staining. Representative images of each isolate are shown. *B. fragilis = Bacteroides*
891 *fragilis; P. intermedia = Prevotella intermedia; C. beijerinckii = Clostridium beijerinckii; R.*
892 *bromii = Ruminococcus bromii; B. infantis = Bifidobacterium longum* subspecies *infantis; E. coli*
893 K12 = *Escherichia coli* K12*; A. muciniphila = Akkermansia muciniphila*. Scale bar shows a width
894 of 10 microns.

895 ***Figure S4. Optimization of EdU-click: EdU concentration***. Mouse fecal bacteria from two
896 independent experiments underwent EdU-click with varying concentrations of EdU and
897 proportions of labeled cells were quantified using flow cytometry. (A) Proportions of EdU+ cells
898 for EdU concentrations from 10 to 100 μM in 15 or 25 μM increments (B) Proportions of EdU+
899 cells for EdU concentrations from 20 to 80 μM in 15 μM increments. Statistical significance
900 determined by Kruskal-Wallis with Dunn's test to correct for multiple comparisons. Comparisons
901 are considered significant at $p \leq 0.05$. (C) Flow cytograms for fecal mouse bacteria incubated with
902 concentrations of EdU from 10-35 μM.

903 ***Figure S5. Rarefaction curves on the number of observed features in each experiment***. The plots
904 below display the rarefaction curves on the number of observed features for (A) the experiment on
905 healthy mice ("Healthy Mice") and (B) the antibiotic perturbation experiment ("Antibiotic
906 Perturbation"), per treatment: Control, Initial; Van = vancomycin, Pmb = polymyxin B. The

907 maximum sequencing depth in each plot was set at the depth at which these sequences were
908 rarefied for alpha and beta diversity analyses.

909 ***Figure S6. Alpha diversity metrics of healthy mice in two independent experiments***. Within-
910 sample alpha diversity plots of the bacterial communities from healthy C57BL/6 mice are shown
911 below, calculated using Shannon's index (A), Simpson Evenness (B), and Observed Features (C)
912 for each experiment. The results from all the sorted fractions (initial and whole community, EdU+
913 and EdU- cells) are combined in these metrics.

914 ***Table SI. Characteristics of mouse fecal-derived bacterial growth curves when exposed to***
915 ***antibiotics***. Mouse fecal-derived bacteria were incubated with or without a cell-membrane specific
916 antibiotic, vancomycin or polymyxin B. The growth curves can be seen in Figure 4a. (A)
917 Numerical summaries of some key characteristics of those growth curves are summarized here.
918 Lag time is here defined as the time it takes until the bacterial community begins its exponential
919 growth phase. Max V = maximum velocity, or maximum replication rate; AUC = area under the
920 curve. (B) P-values comparing Condition 1 versus Condition 2 for all growth curve characteristics.
921 All values were calculated in the EPOCH2 software and statistical analyses were done in GraphPad
922 Prism using a one-way ANOVA with Dunnett's test to correct for multiple comparisons,
923 comparing the control to each treatment.

924 ***Table SII. Potential vancomycin resistance genes in an* Ileibacterium valens *strain***. The protein
925 sequences of a publicly available genome for *Ileibacterium valens* (see the main text) were run
926 through the Comprehensive Antibiotic Resistance Database (CARD) Resistance Gene Identifier
927 (RGI) to detect antibiotic resistance genes. Only those for vancomycin and related glycopeptide
928 antibiotics are shown. Note that all hits shown are classified as "Loose" hits.

929 **Figures**

930 Figure 1

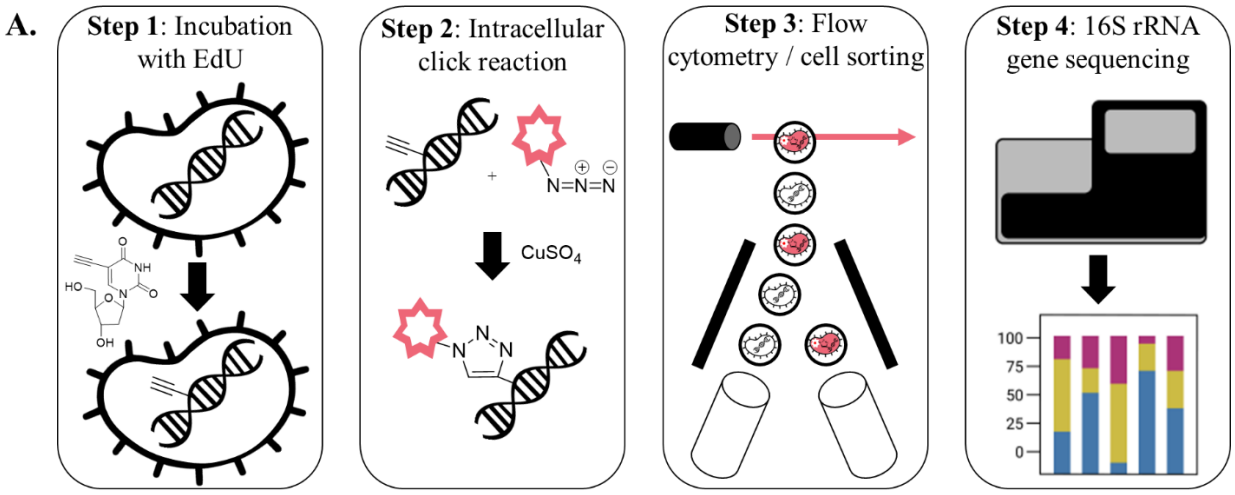

931

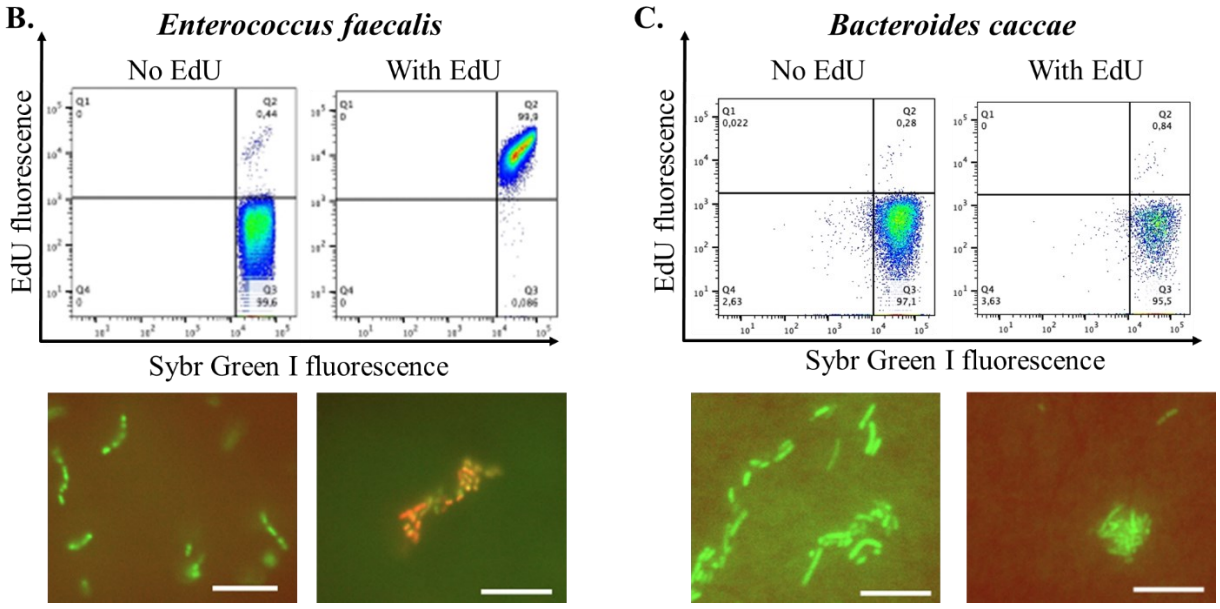

932

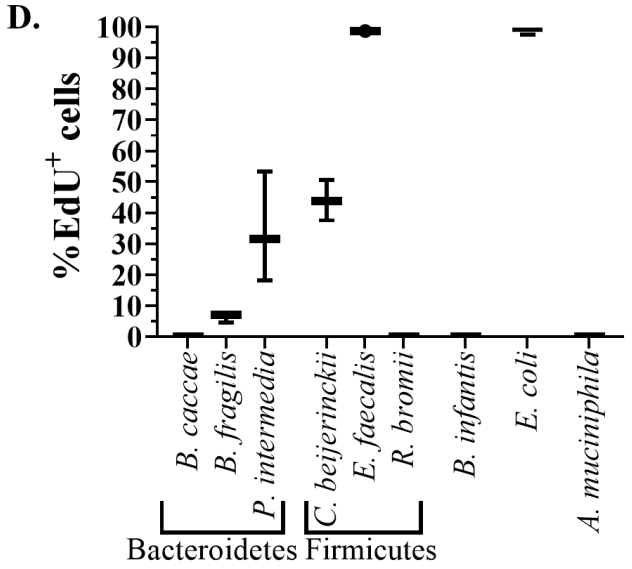

933

934 Figure 2

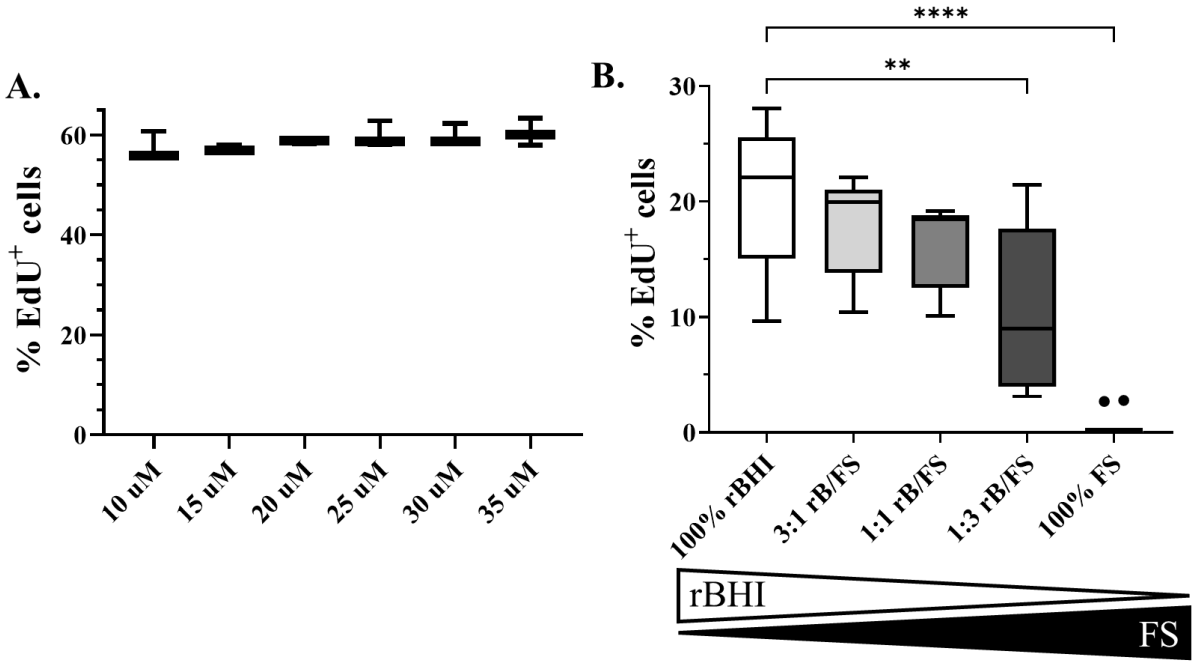

935

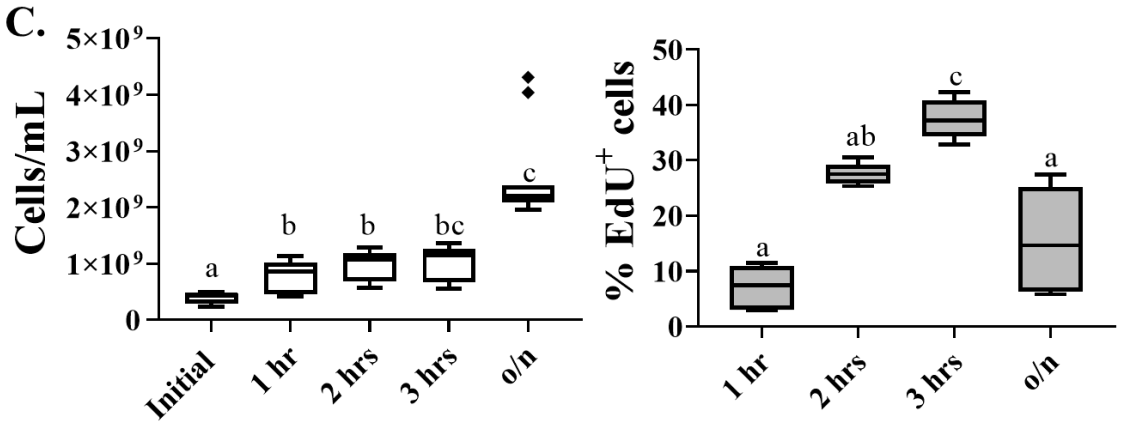

936

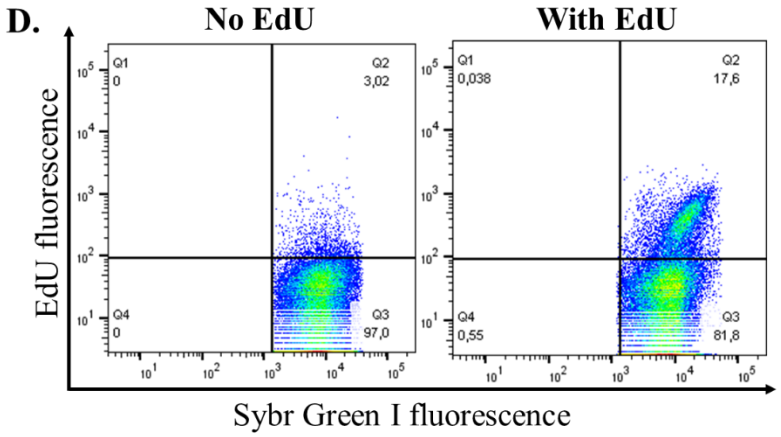

937

938 Figure 3

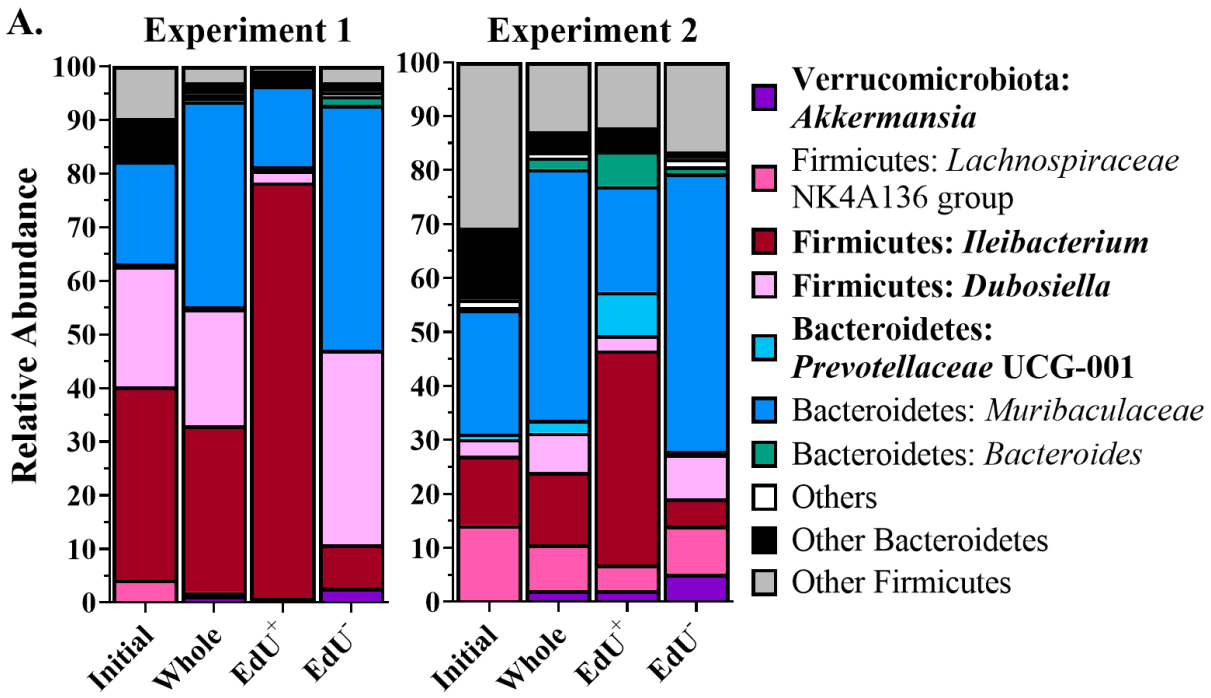
A.
Experiment 1
Experiment 2
Relative Abundance
100
90
80
70
60
50
40
30
20
10
0
Initial
Whole
EdU+
EdU-
Verrucomicrobiota: Akkermansia
Firmicutes: Lachnospiraceae NK4A136 group
Firmicutes: Ileibacterium
Firmicutes: Dubosiella
Bacteroidetes: Prevotellaceae UCG-001
Bacteroidetes: Muribaculaceae
Bacteroidetes: Bacteroides
Others
Other Bacteroidetes
Other Firmicutes

939

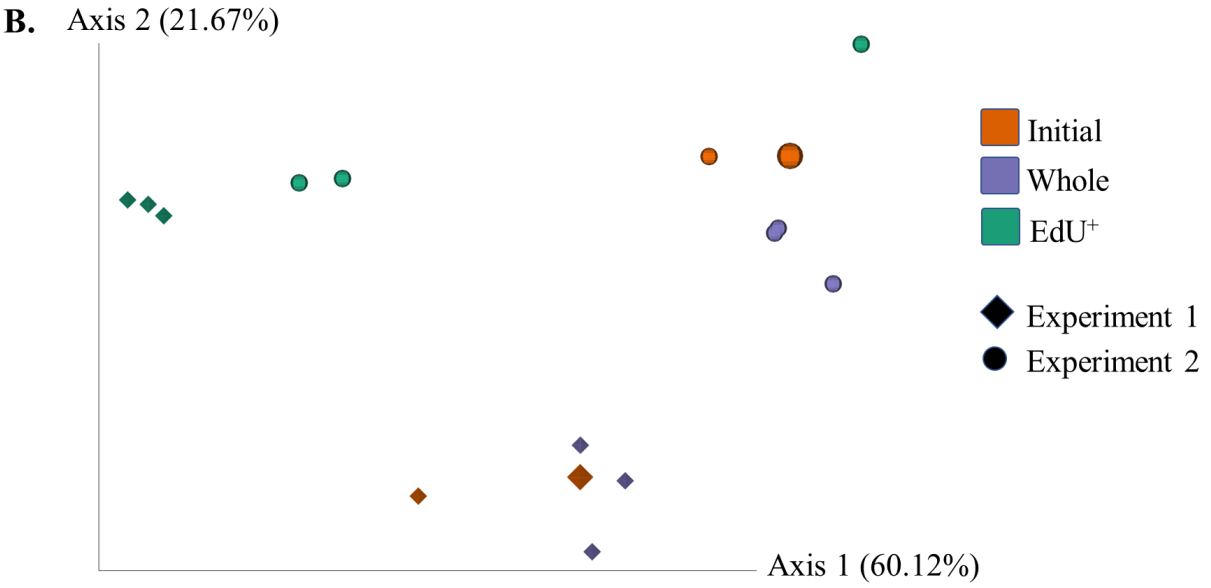
B.
Axis 2 (21.67%)
Axis 1 (60.12%)
Initial
Whole
EdU+
Experiment 1
Experiment 2

940

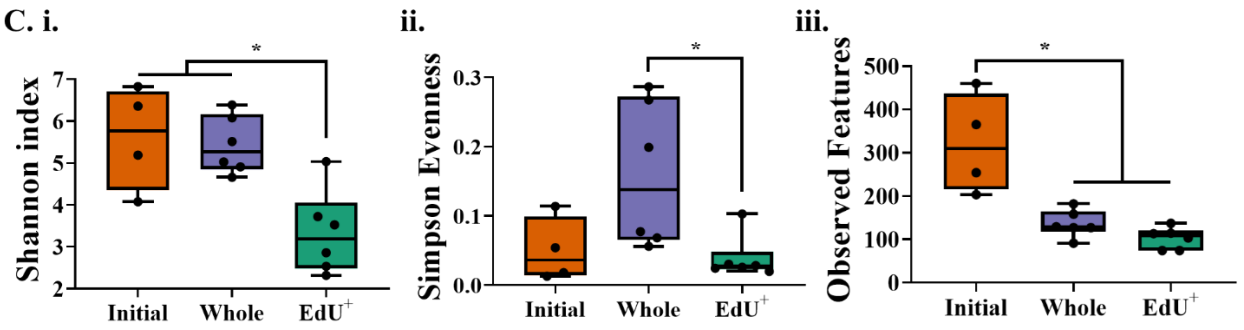

941

942 Figure 4

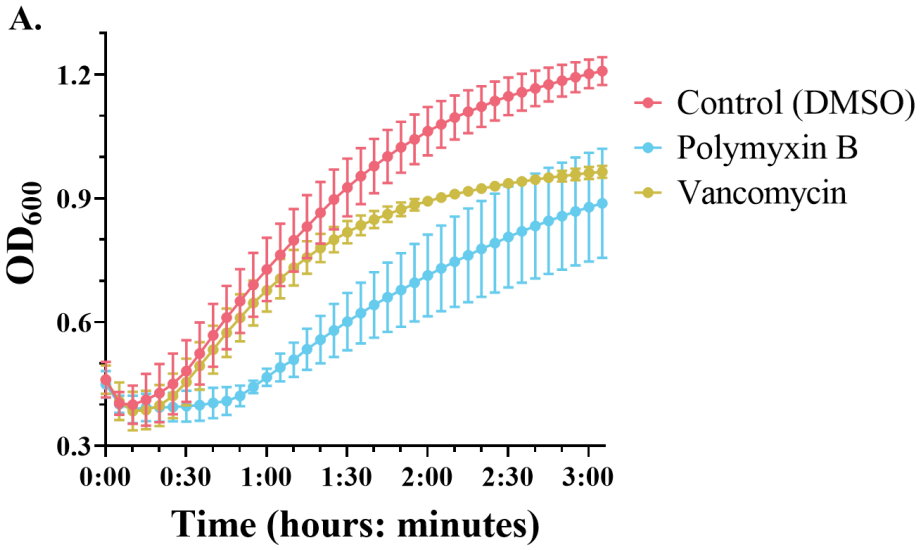

943

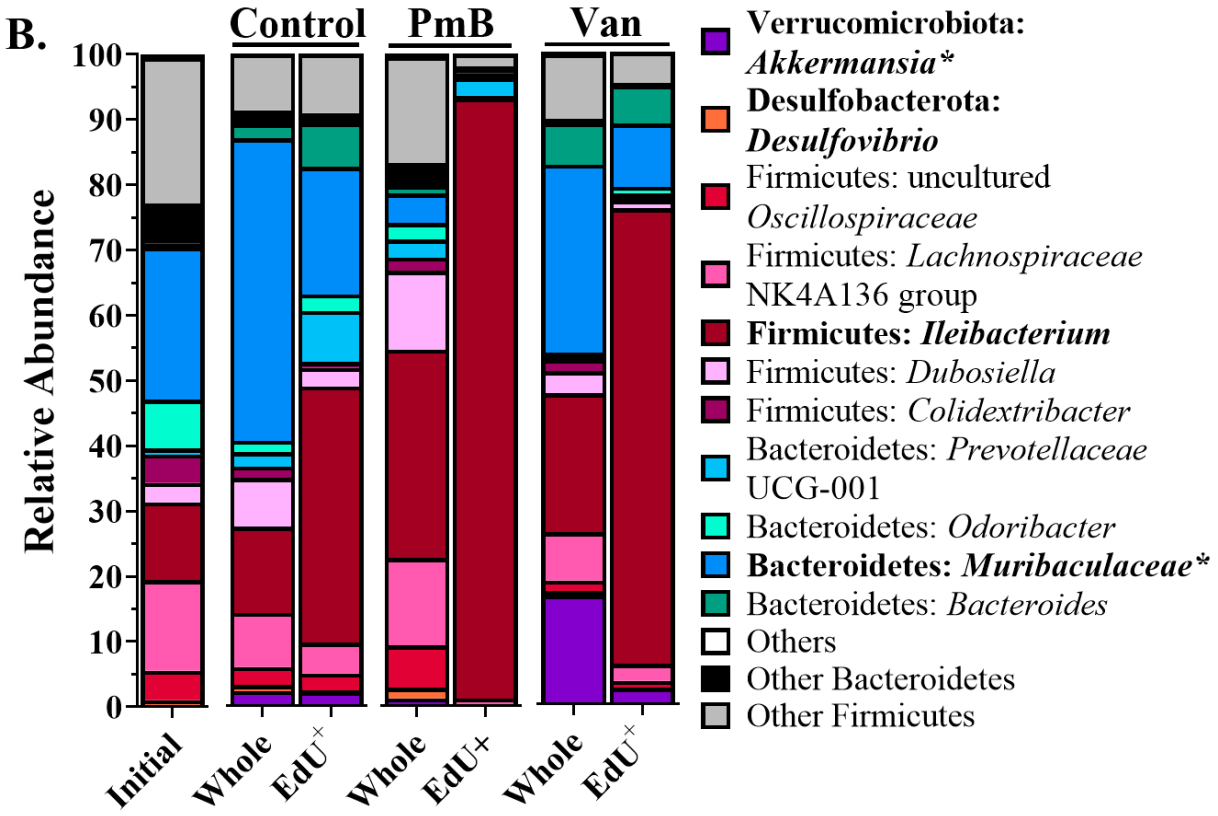
B.
Control
PmB
Van
Relative Abundance
100
90
80
70
60
50
40
30
20
10
0
Initial
Whole
EdU+
Whole
EdU+
Whole
EdU+
Verrucomicrobiota: Akkermansia*
Desulfobacterota: Desulfovibrio
Firmicutes: uncultured Oscillospiraceae
Firmicutes: Lachnospiraceae NK4A136 group
Firmicutes: Ileibacterium
Firmicutes: Dubosiella
Firmicutes: Colidextribacter
Bacteroidetes: Prevotellaceae UCG-001
Bacteroidetes: Odoribacter
Bacteroidetes: Muribaculaceae*
Bacteroidetes: Bacteroides
Others
Other Bacteroidetes
Other Firmicutes

944

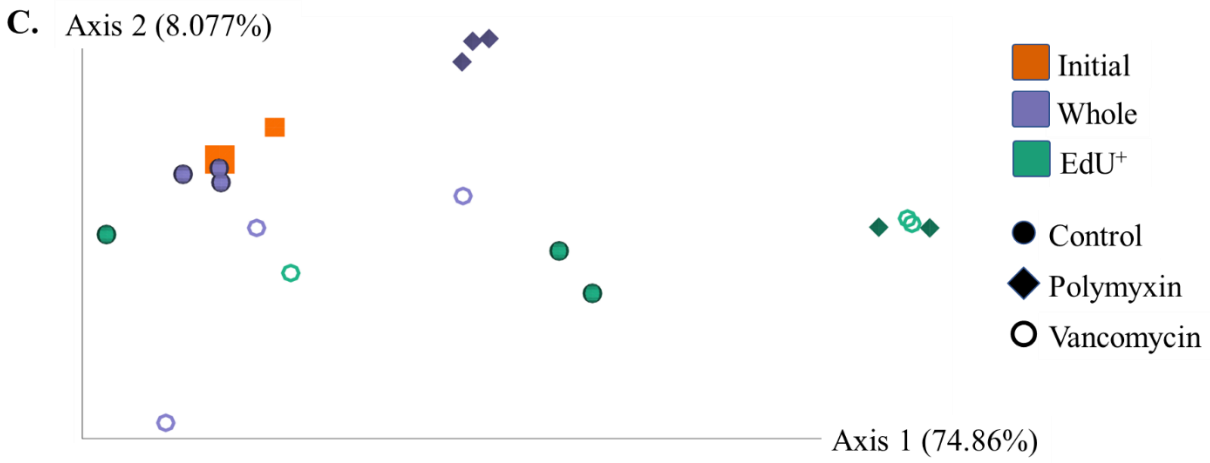
C.
Axis 2 (8.077%)
Axis 1 (74.86%)
Initial
Whole
EdU+
Control
Polymyxin
Vancomycin

945

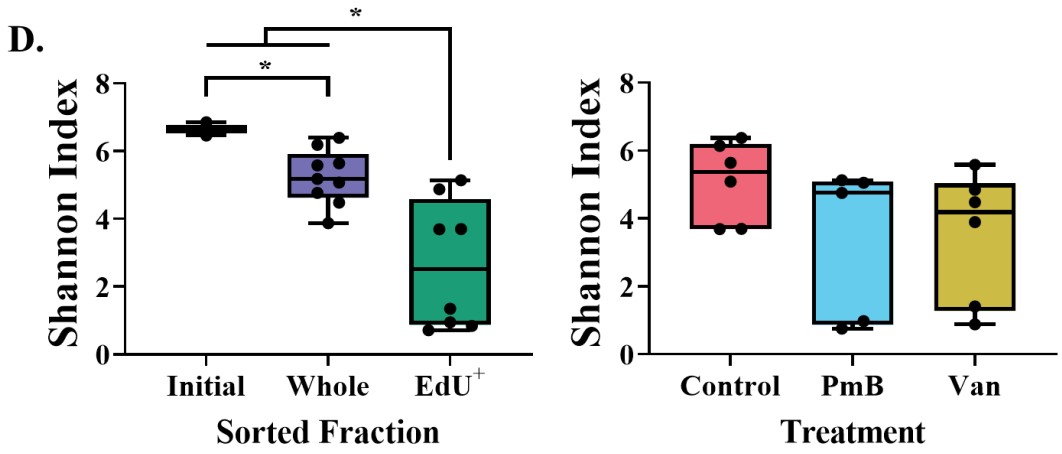

946

947 **Supplemental Figures**

948 Fig S1

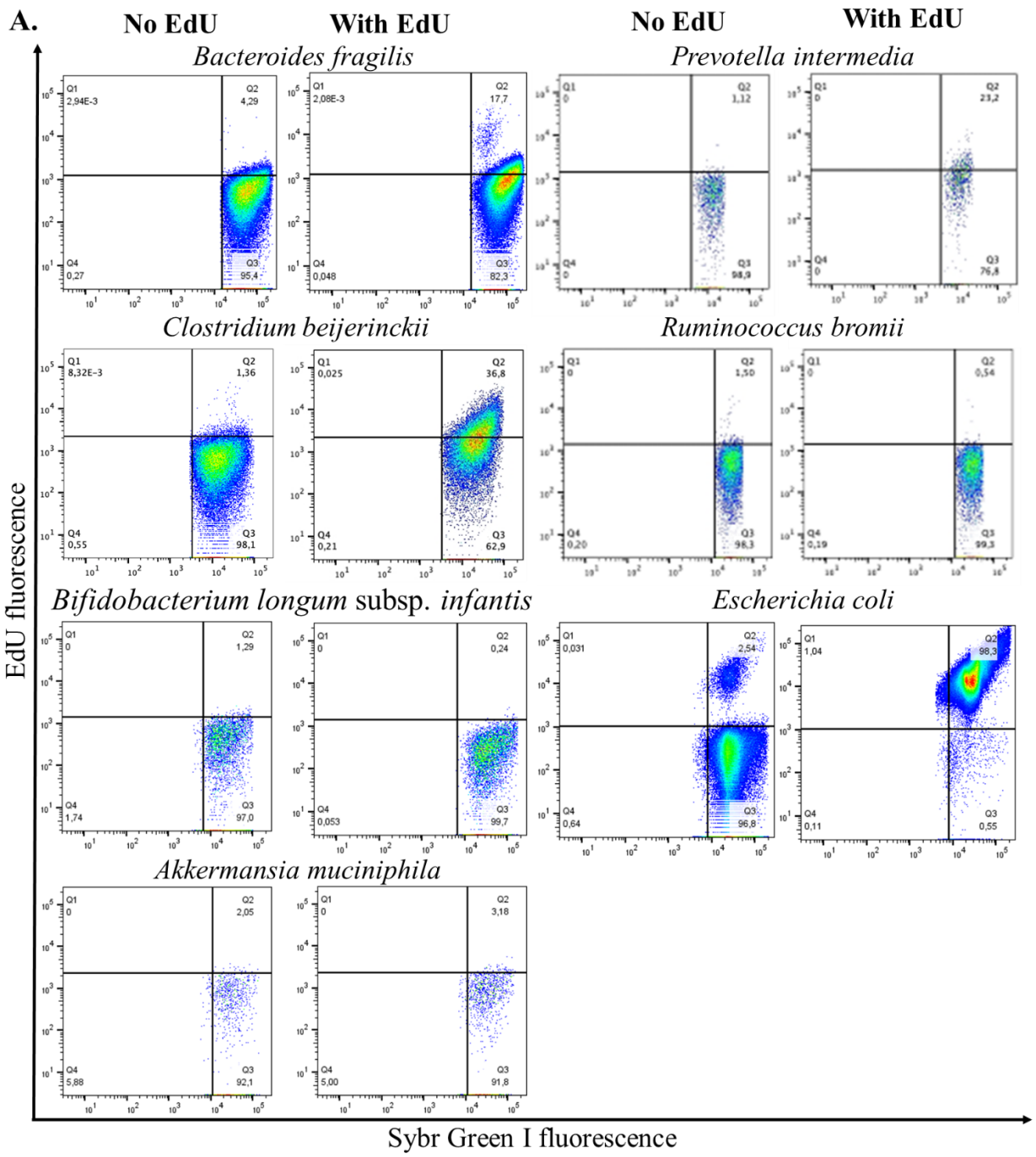
A.
No EdU
With EdU
No EdU
With EdU
Bacteroides fragilis
Prevotella intermedia
Clostridium beijerinckii
Ruminococcus bromii
Bifidobacterium longum subsp. infantis
Escherichia coli
Akkermansia muciniphila
EdU fluorescence
Sybr Green I fluorescence

949

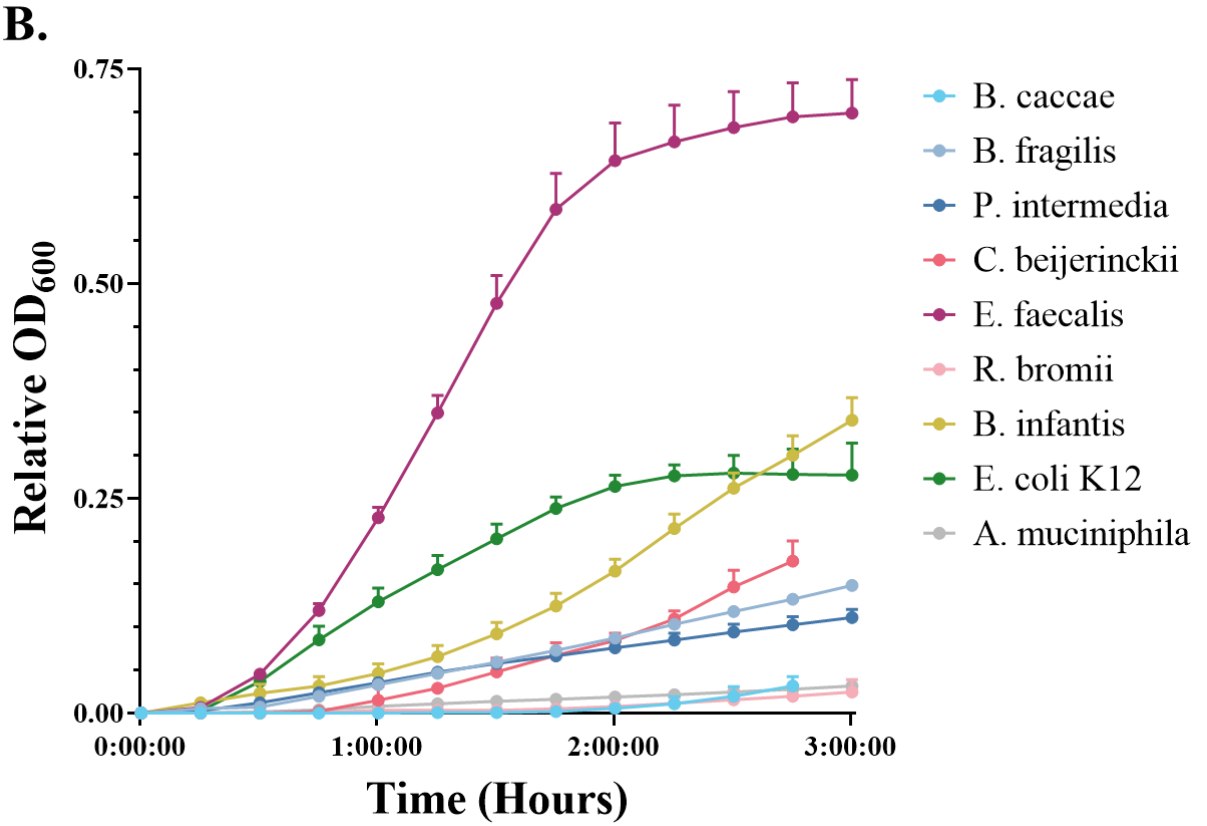

950

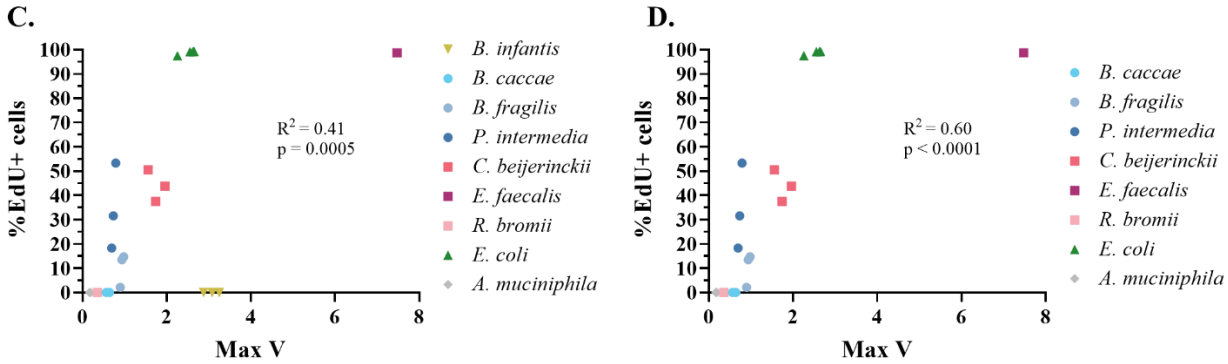

951

952 Fig S2

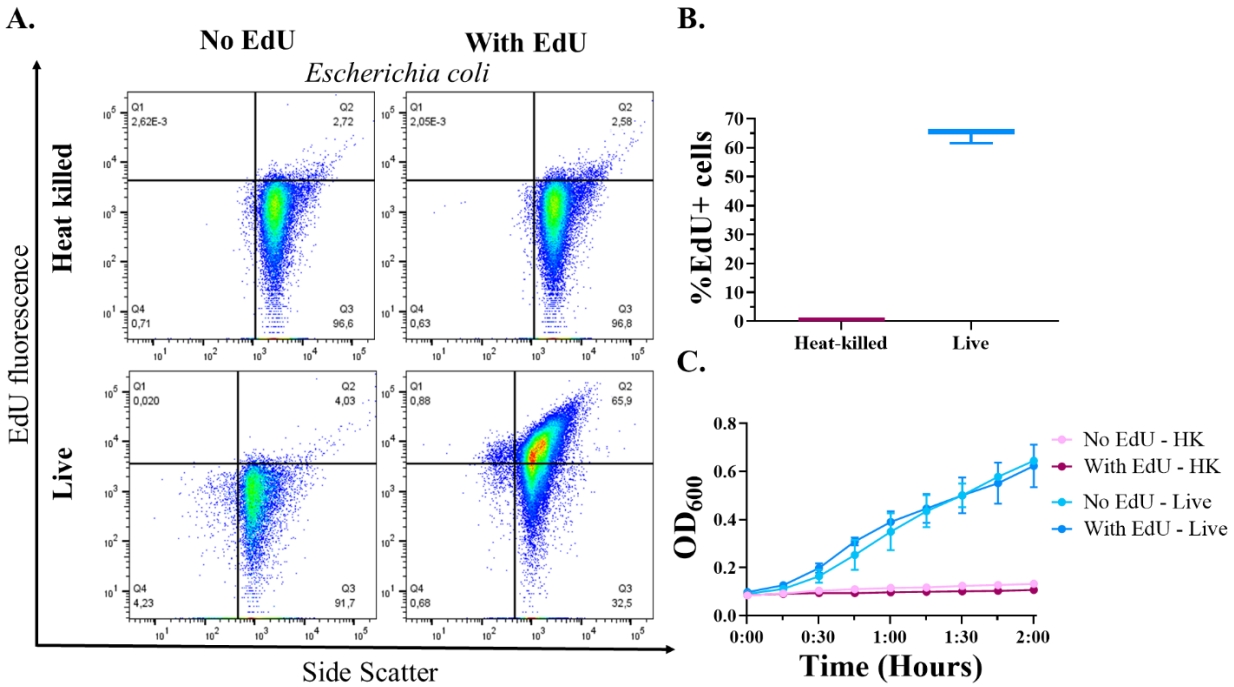

953

954 Fig S3

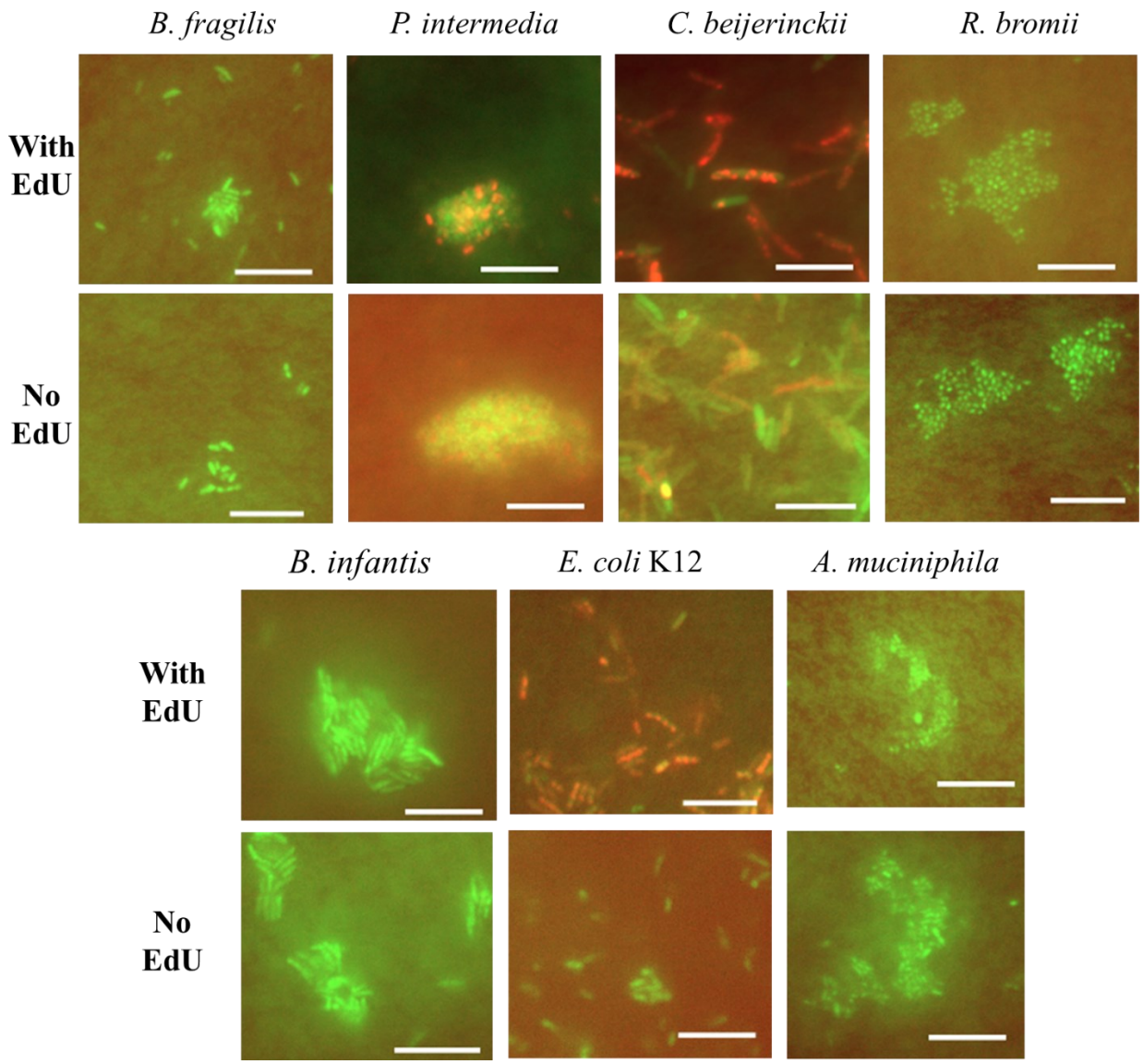

955

956 Fig S4

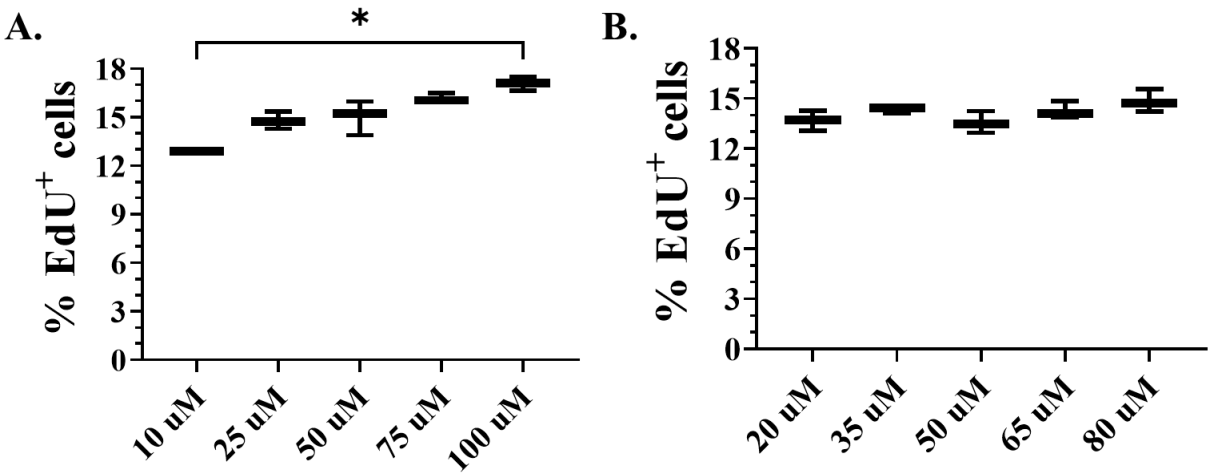

957

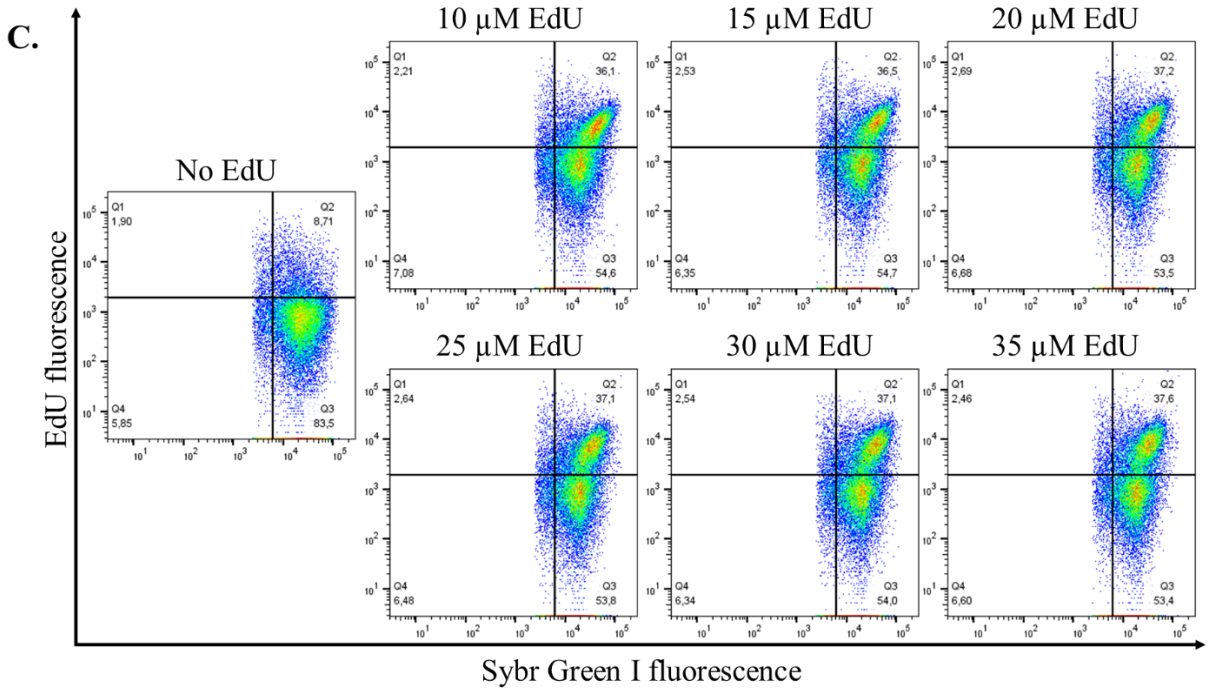

958

959 Fig S5

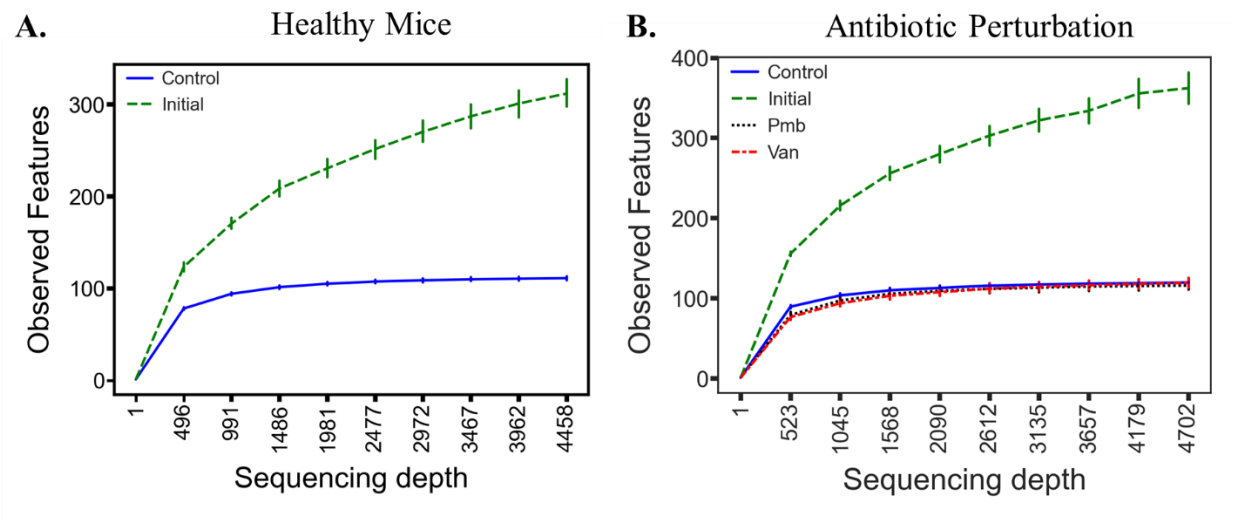

Fig S6

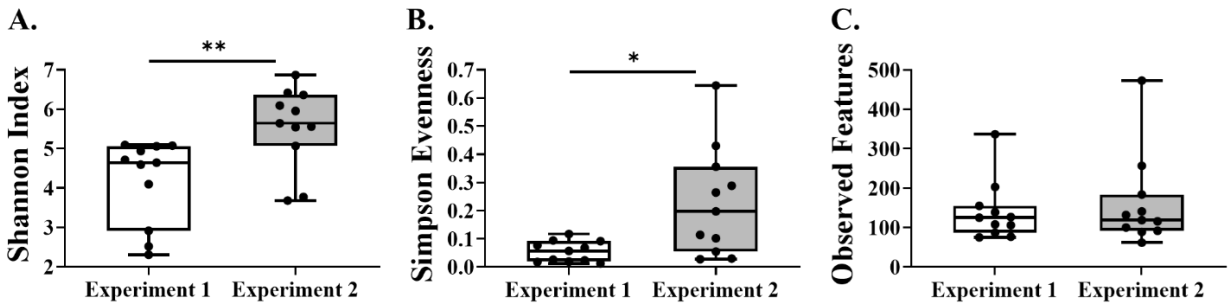

Table SIA

Condition	Replicate	Lag Time (HH:MM:SS)	Max V	AUC
Control	1	00:23:43	8.375	2.844
	2	00:31:19	8.143	2.478
	3	00:27:58	9.039	2.701
Vancomycin	1	00:45:07	7.607	2.223

	2	00:40:07	8.935	2.359
	3	00:35:07	7.214	2.346
Polymyxin B	1	01:25:07	3.011	1.683
	2	00:55:07	6.587	1.958
	3	01:00:07	5.785	2.002

964

965 Table SIB

Condition 1	**Condition 2**	**Lag Time**	**Max V**	**AUC**
Control	Vancomycin	P = 0.8807	P = 0.7836	**P = 0.0455**
	Polymyxin B	**P = 0.0073**	**P = 0.0264**	**P = 0.0013**

966

967 Table SII

Antibiotic Resistance Ontology (ARO) Term	**Antimicrobial Resistance (AMR) Gene Family**	**Drug Class**	**Resistance Mechanism**	**% Identity of Matching Region**	**% Length of Reference Sequence**
vanN	glycopeptide resistance gene cluster, Van ligase	glycopeptide antibiotic	antibiotic target alteration	29.41	121.28

vanG	glycopeptide resistance gene cluster, Van ligase	glycopeptide antibiotic	antibiotic target alteration	40.34	100.57
vanK gene in vanI cluster	glycopeptide resistance gene cluster, vanK	glycopeptide antibiotic	antibiotic target alteration	25.29	103.73
vanR gene in vanA cluster	glycopeptide resistance gene cluster, vanR	glycopeptide antibiotic	antibiotic target alteration	29.9	45.02
vanR gene in vanF cluster	glycopeptide resistance gene cluster, vanR	glycopeptide antibiotic	antibiotic target alteration	41.67	102.60
vanR gene in vanB cluster	glycopeptide resistance gene cluster, vanR	glycopeptide antibiotic	antibiotic target alteration	29.79	75.45
vanR gene in vanF cluster	glycopeptide resistance gene cluster, vanR	glycopeptide antibiotic	antibiotic target alteration	30.7	97.40
vanR gene in vanL cluster	glycopeptide resistance gene cluster, vanR	glycopeptide antibiotic	antibiotic target alteration	34.82	94.81

vanR gene in vanF cluster	glycopeptide resistance gene cluster, vanR	glycopeptide antibiotic	antibiotic target alteration	40.0	103.90
vanR gene in vanN cluster	glycopeptide resistance gene cluster, vanR	glycopeptide antibiotic	antibiotic target alteration	34.65	96.52
vanT gene in vanG cluster	glycopeptide resistance gene cluster, vanT	glycopeptide antibiotic	antibiotic target alteration	38.27	55.06
vanT gene in vanG cluster	glycopeptide resistance gene cluster, vanT	glycopeptide antibiotic	antibiotic target alteration	36.12	47.47
vanU gene in vanG cluster	glycopeptide resistance gene cluster, vanU	glycopeptide antibiotic	antibiotic target alteration	35.48	97.33
vanH gene in vanB cluster	vanH, glycopeptide resistance gene cluster	glycopeptide antibiotic	antibiotic target alteration	26.14	119.81
vanH gene in vanA cluster	vanH, glycopeptide	glycopeptide antibiotic	antibiotic target alteration	35.29	88.20

	resistance gene cluster				
vanS gene in vanF cluster	vanS, glycopeptide resistance gene cluster	glycopeptide antibiotic	antibiotic target alteration	28.14	208.77
vanS gene in vanM cluster	vanS, glycopeptide resistance gene cluster	glycopeptide antibiotic	antibiotic target alteration	27.95	196.76
vanS gene in vanF cluster	vanS, glycopeptide resistance gene cluster	glycopeptide antibiotic	antibiotic target alteration	22.01	89.04
vanY gene in vanF cluster	vanY, glycopeptide resistance gene cluster	glycopeptide antibiotic	antibiotic target alteration	29.09	114.33
vanY gene in vanF cluster	vanY, glycopeptide	glycopeptide antibiotic	antibiotic target alteration	41.48	110.92

	resistance gene cluster				
vanZ gene in vanF cluster	vanZ, glycopeptide resistance gene cluster	glycopeptide antibiotic	antibiotic target alteration	28.49	178.64

968